Measurement of B production fraction ratio using Run 2 B parking dataset at CMS

Taeun Kwon

Brown University

Lepton-Photon 2025 at Madison, Wisconsin
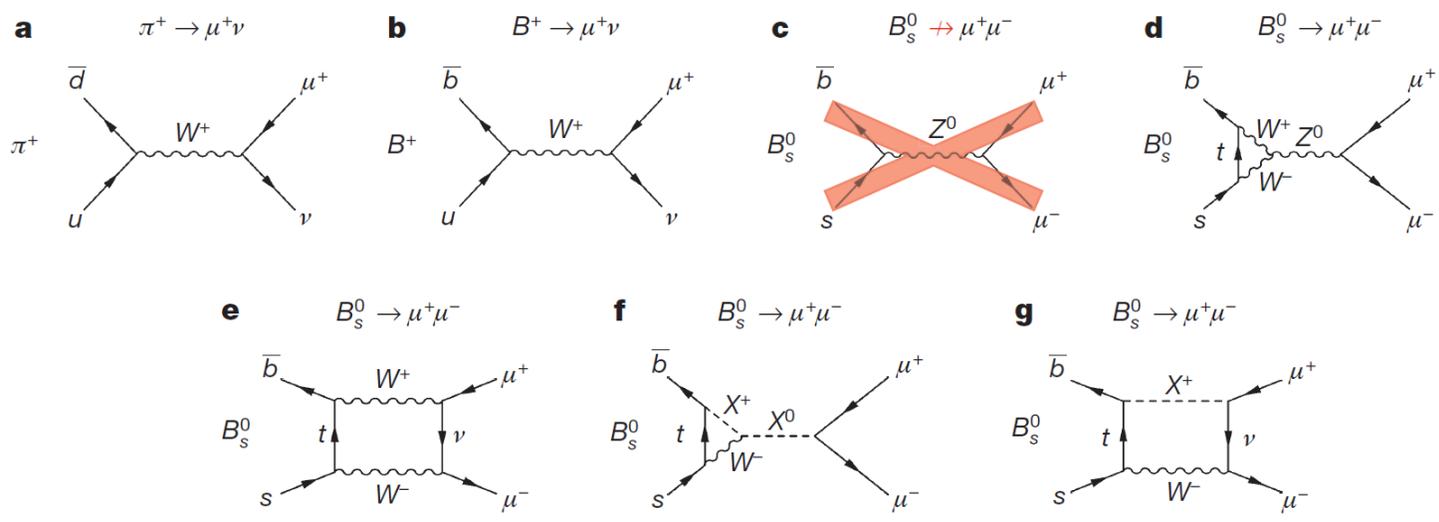25th-29th August 2025

The Production fractions (f_u, f_s, f_d)

- Probabilities for a b quark to hadronize into a B^+, B_s, B^0 meson

Production fraction ratio (PFR)

- Necessary input for branching fraction measurements of B_s^0 channels

- $\mathcal{B}(B_s \to \mu^+\mu^-) = \dfrac{f_u}{f_s} \cdot \dfrac{N_{sig}}{N(B^\pm \to J/\Psi K^\pm)} \cdot \mathcal{B}(B^\pm \to J/\Psi K^\pm) \cdot \dfrac{\varepsilon(B^\pm)}{\varepsilon(B_s)}$

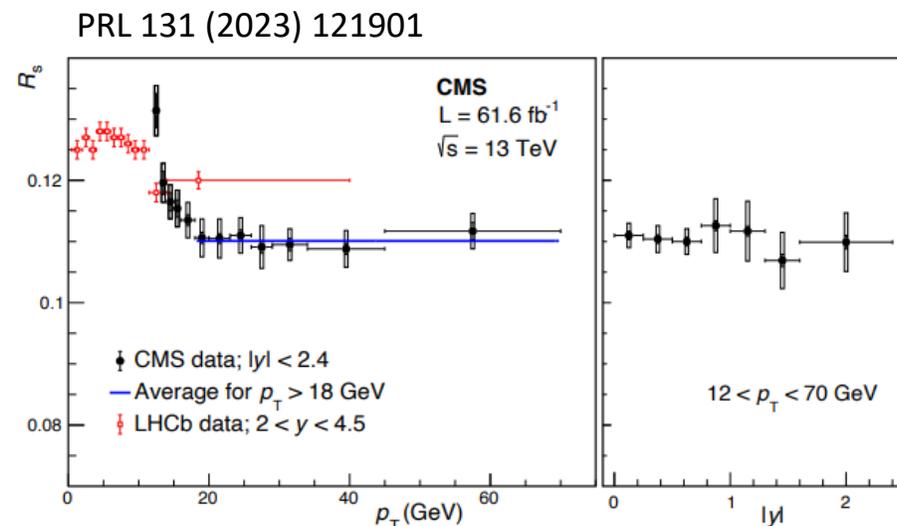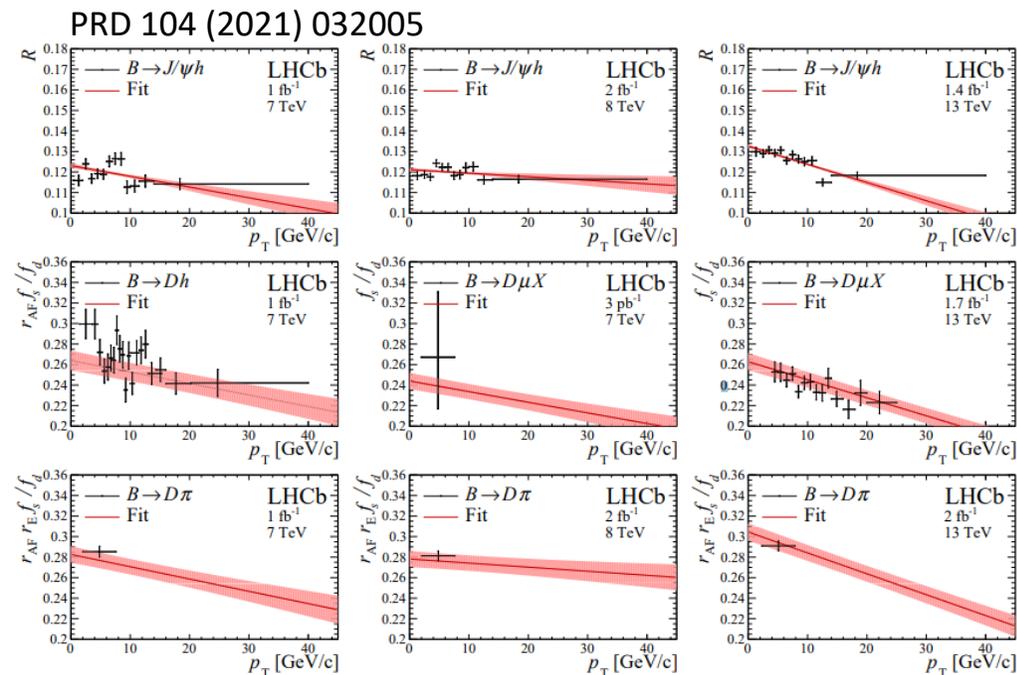- **Systematics are dominated by the uncertainty of f_s/f_u**

Previous measurements in LHCb & CMS

- **LHCb** has measured PFRs in many different channels
  - Measurements performed in the forward rapidity region(2 < y < 4.5)
- **CMS** only had the result which uses **charmonium channels**
  - This only can be **a relative measurement** as $\mathcal{B}(B_s \to J/\Psi\phi)$ is dependent on the previous measurement of f_s/f_d

➢ **Measure PFRs in open-charm decays first time at CMS**

- $B^{\pm} \to \pi^{\pm}\overline{D}^0(K^+\pi^-), B_s^0 \to \pi^+D_s^-\left(\pi^-\varphi(K^+K^-)\right), B^0 \to \pi^+D^-(K^+\pi^-\pi^-)$
- $B_s^0 \to \pi^+D_s^-$ branching fraction is theoretically well understood

PRD 104 (2021) 032005

PRL 131 (2023) 121901
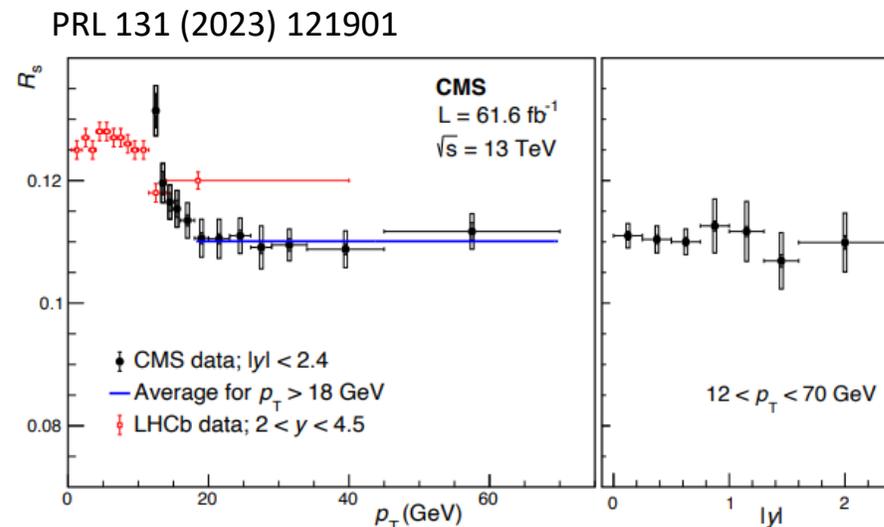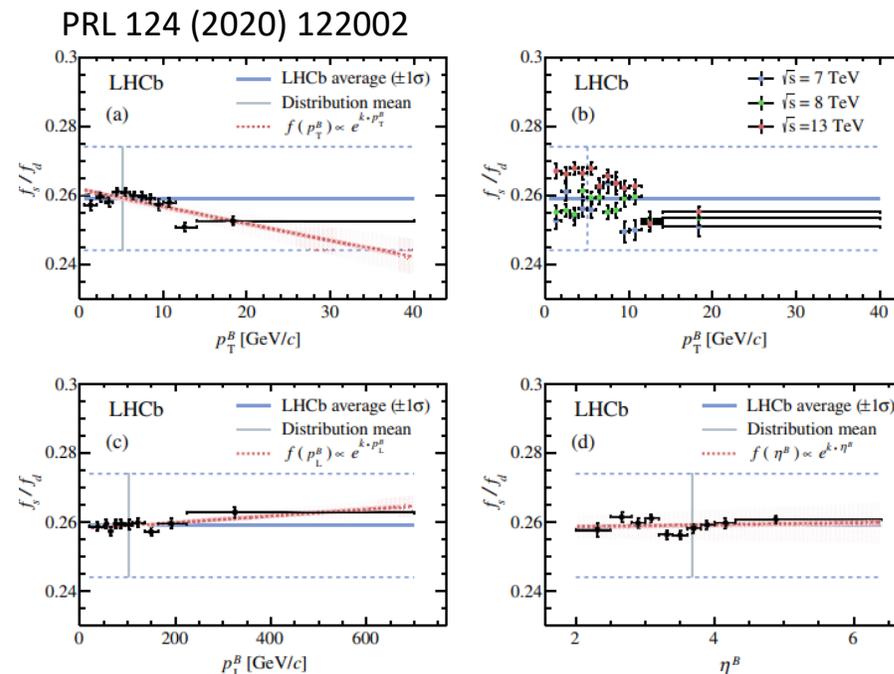
LHCb has continuously seen p_T dependence of f_s/f_d:

- $f_s/f_d(p_T, 13 \text{ TeV}) = (0.263 \pm 0.008) + ((-17.6 \pm 2.1)\times 10^{-4}) \cdot p_T$
- With a significance of 6.0σ with respect to the constant hypothesis

Previous CMS study has also seen the p_T dependence of f_s/f_u in low p_T

- The trend is consistent with LHCb measurement, but **not linear**
- Asymptotically constant at large p_T (p_T > 18 GeV)

No rapidity dependence is observed both in LHCb and CMS

➢ **Test the dependency of PFRs on p_T**

PRL 124 (2020) 122002

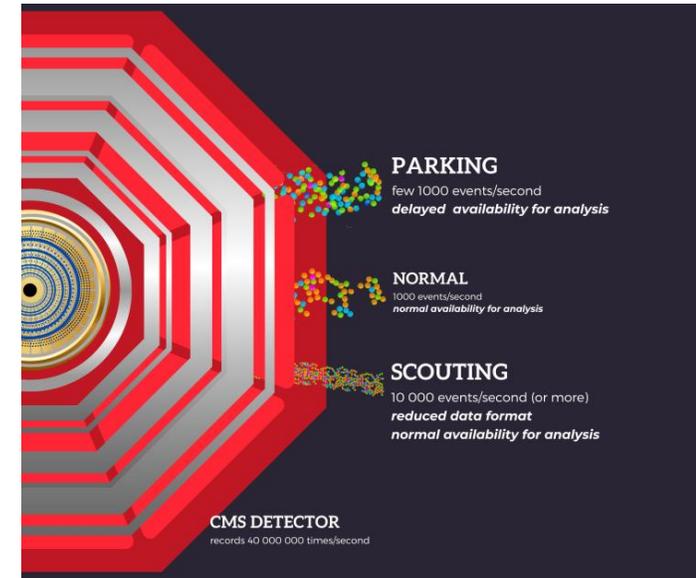PRL 131 (2023) 121901

B parking dataset during Run 2

CMS introduced a new trigger strategy, "data parking," for B physics studies

- Data parking stores full event content for later reconstruction
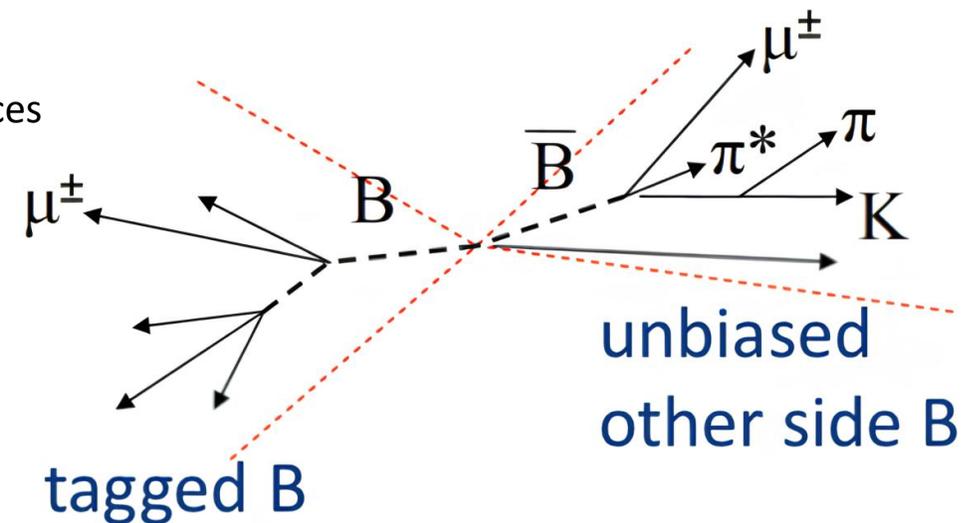- Data parking dedicated to B physics first introduced in 2018

10 billions of unbiased B events collected during Run 2

- Purity ~ 75%
- Access to decay modes down to $O(10^{-7})$ branching fraction
- L = 41.6 / fb

Trigger strategy:

- B hadrons travel before decaying, producing displaced secondary vertices
- Triggers select one single displaced muon from one B hadron (**tag side**)
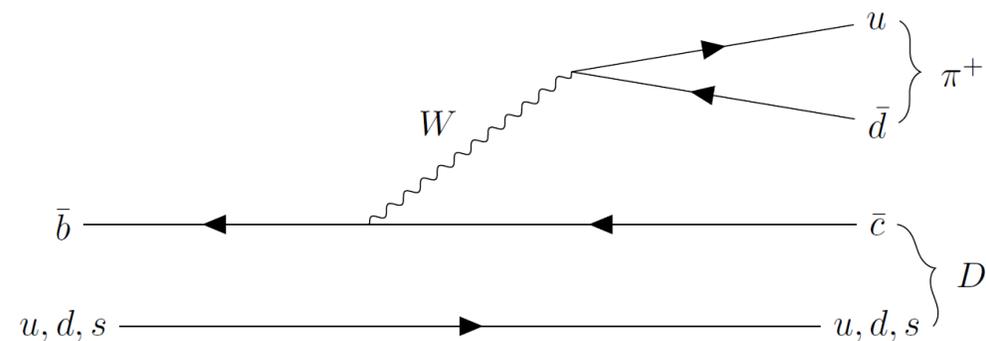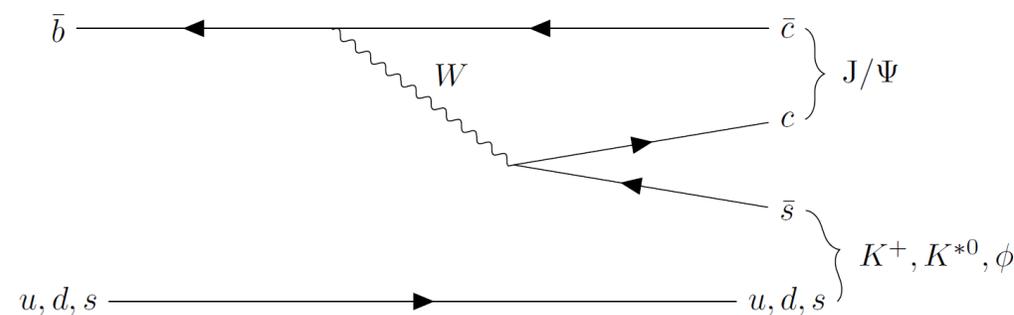- The opposite B hadron (**probe side**) remains unbiased

Analysis Strategy

Channels

- **Open-charm decays**:
  - $B^{\pm} \to \pi^{\pm}\overline{D}^0(K^+\pi^-), B_s^0 \to \pi^+ D_s^-\left(\pi^-\varphi(K^+K^-)\right), B^0 \to \pi^+ D^-(K^+\pi^-\pi^-)$
  - Using probe-side
- **Charmonium decays**:
  - $B^{\pm} \to J/\Psi(1S)K^{\pm}, B_s \to J/\Psi(1S)\phi(\to KK), B^0 \to J/\Psi(1S)K^*(\to K\pi)$
  - Using both probe and tag side

(a) Open-charm decays

What to measure:

1. The measurement of **absolute PFRs, f_s/f_u and f_s/f_d** using **open-charm**
   - First at CMS
2. Dependency test of **f_s/f_u and f_s/f_d** using **charmonium**
   - Through **the relative PFR, $\mathcal{R}_s$ and $\mathcal{R}_s^d$**
3. Measurement of **f_d/f_u** using **both channels**
   - Explicit measurement without assuming isospin invariance
4. Measurement of the **normalization from Charmonium ($\mathcal{R}_s$ and $\mathcal{R}_s^d$) to hadronic open-charm (f_s/f_u, and f_s/f_d)**
   - **c_{su} and c_{sd}**
   - Global constant independent of p_T dependence of PFRs

(b) Charmonium decays

Channels:

- $B^+ \to \pi^+ \overline{D}^0 (K^+\pi^-)$
- $B_s^0 \to \pi^+ D_s^- (\pi^- \varphi(K^+K^-))$
- $B^0 \to \pi^+ D^- (K^+\pi^-\pi^-)$

Key Equation:

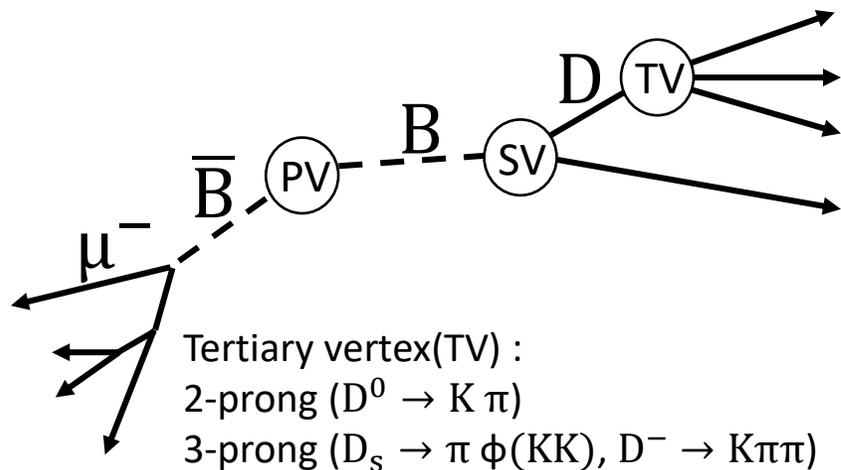- $$\frac{f_s}{f_d} = \frac{\mathcal{B}(B^0\to\pi^+D^-)}{\mathcal{B}(B_s^0\to\pi^+D_s^-)} \frac{\mathcal{B}(D^-\to K^+\pi^-\pi^-)}{\mathcal{B}(D_s^-\to\pi^-\varphi(K^+K^-))} \frac{N_{corr}(B_s^0)}{N_{corr}(B^0)}$$

$$= \frac{\mathcal{B}(B^0\to K^+D^-)}{\mathcal{B}(B_s^0\to\pi^+D_s^-)} \frac{\mathcal{B}(B^0\to\pi^+D^-)}{\mathcal{B}(B^0\to K^+D^-)} \frac{\mathcal{B}(D^-\to K^+\pi^-\pi^-)}{\mathcal{B}(D_s^-\to\pi^-\varphi(K^+K^-))} \frac{N_{corr}(B_s^0)}{N_{corr}(B^0)}$$

$$= \Phi_{PS} \left|\frac{V_{us}}{V_{ud}}\right|^2 \left(\frac{f_K}{f_\pi}\right)^2 \frac{\tau_{B^0}}{\tau_{B_s^0}} \frac{1}{N_a N_F} \frac{\mathcal{B}(B^0\to\pi^+D^-)}{\mathcal{B}(B^0\to K^+D^-)} \frac{\mathcal{B}(D^-\to K^+\pi^-\pi^-)}{\mathcal{B}(D_s^-\to\pi^-\varphi(K^+K^-))} \frac{N_{corr}(B_s^0)}{N_{corr}(B^0)}$$

Inputs	Description	Value
Φ_{PS}	The difference in phase space of two channels	1.003 [PDG]
$\dfrac{|V_{us}|f_K}{|V_{ud}|f_\pi}$	Product of CKM matrix and decay constant ratios	0.2768 [PRD 100 (2019) 034514]
$\tau_{B_s^0}/\tau_{B^0}$	Lifetime ratio between B^0 and B_s^0	1.002 ± 0.003 [HFLAV]
$1/N_a$	The ratio of correction accounting for non-factorizable effect	$1.0048^{+0.0046}_{-0.0022}$ [EPJC 80 (2020) 347 and 951]
$1/N_F$	The ratio of form factors	1.002 ± 0.042 [EPJC 80 (2020) 347 and 951]

Prediction of $\mathcal{B}(B^0 \to K^+D^-)/\mathcal{B}(B_s^0 \to \pi^+D_s^-)$ with external theory inputs

1) $\mathcal{B}(B_s^0 \to \pi^+D_s^-)$ also dominated by LHCb studies (and dependent on f_s/f_d)
2) $\mathcal{B}(B^0 \to K^+D^-)$ **has a more theoretically clean prediction than $B^0 \to \pi^+D^-$**, but **Cabibbo-suppressed**
3) **N($B^0 \to \pi^+D^-$) used as a proxy** to improve statistics
   - $\mathcal{B}(B^0 \to K^+D^-)/\mathcal{B}(B^0 \to \pi^+D^-) = 0.0819 \pm 0.0020$, measured with a good precision

Selection criteria

Tracks
- $p_T > 1$ GeV, $|\eta| < 2.4$, $|\Delta z(\text{trk}, \text{trg } \mu)| < 0.5$ cm, DCA significance > 1
- $\Delta R(\text{trk}, \text{trg } \mu) > 0.4$, probe side selection
- Each track is considered either K or π (mass assignment)

Tertiary vertex (D^0, D_s, D^-)
- Prob(TV) > 0.01, L_{xy} significance > 5
- Leading track $p_T > 1.5$ GeV

Secondary vertex (B^+, B_s^0, B^0)
- $\cos\alpha$ 2D > 0.999, L_{xy} significance > 7
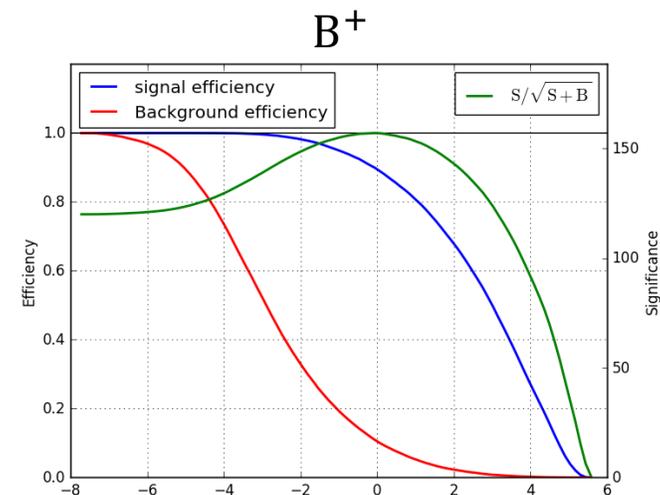- p_T of track directly from B > 1.5 GeV
- * In B_s^0, background subtraction is performed in $m(K^+K^-)$ to reject non-ϕ resonance

- B^+, B^0 :
  - $|m(\text{TV}) - m(D)| < 20$ MeV
- B_s^0:
  - $|m(\text{TV}) - m(D)| < 15$ MeV
  - $|m(K^+K^-) - m(\phi)| < 10$ MeV

Tertiary vertex(TV) :
2-prong ($D^0 \to K\pi$)
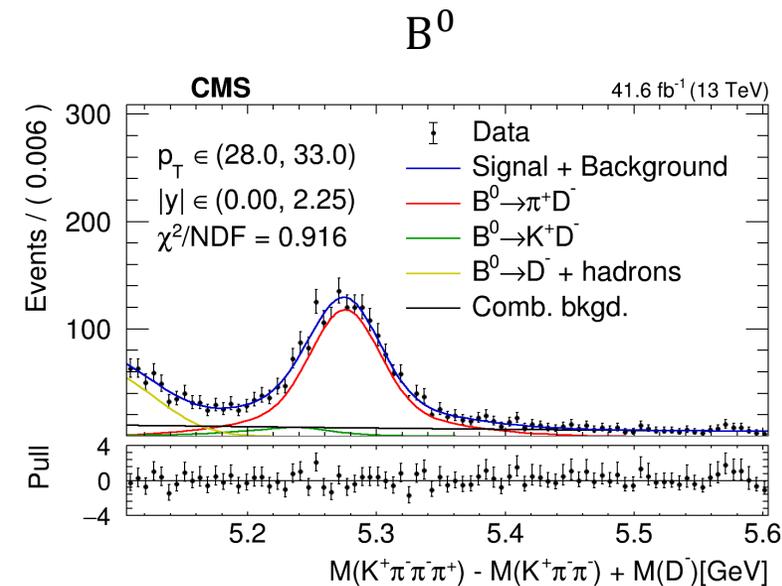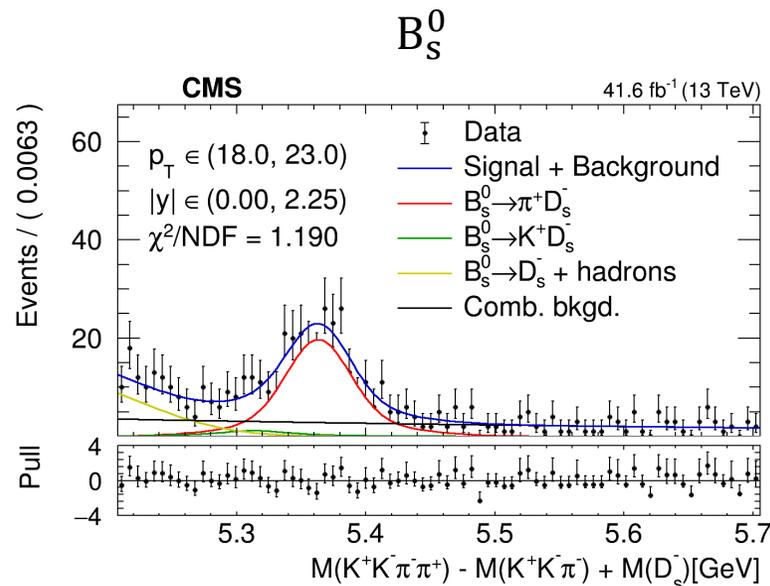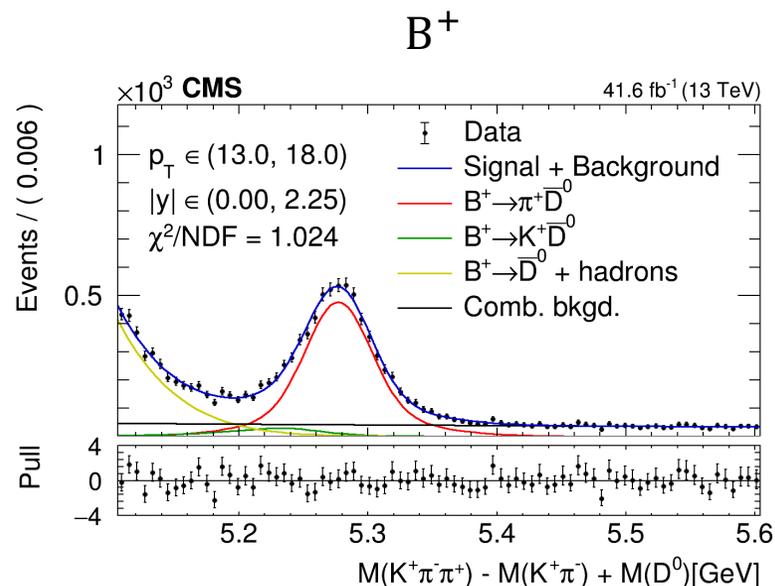3-prong ($D_s \to \pi\phi(KK)$, $D^- \to K\pi\pi$)

BDT is trained for the further optimization of $S/\sqrt{S+B}$

- BDT threshold is chosen to maximize the $S/\sqrt{S+B}$

Only the right sideband, dominated by combinatorial background is considered

- Dominant background in signal region

Fit is done on the **invariant mass distribution of B candidates, corrected by M(D$_{cand}$) - M(D$_{true}$)** to improve the resolution

$$PDF(x) = N_{primary} \cdot \left(\frac{f}{\sigma_1 \sqrt{2\pi}} \cdot \exp\left(-\frac{1}{2}\frac{(x-\mu)^2}{\sigma_1^2}\right) + \frac{1-f}{\sigma_2 \sqrt{2\pi}} \cdot \exp\left(-\frac{1}{2}\frac{(x-\mu)^2}{\sigma_2^2}\right) \right)$$

Signal

$$+ R_{K/\pi} \cdot N_{primary} \cdot \frac{\delta}{\lambda\sqrt{2\pi}} \frac{1}{\sqrt{(1+(\frac{x-\eta}{\lambda})^2)}} \exp\left(-\frac{1}{2}(\gamma + \delta\sinh^{-1}(\frac{x-\eta}{\lambda}))^2\right)$$

Bkg – B → KD

$$+ N_{partial\ reco} \cdot erf\left(\frac{(x-\mu)}{\sigma}\right)$$

Bkg – partially reconstructed

$$+ N_{combinatorial} \cdot \exp(b \cdot x)$$

Bkg – combinatorial

Source	Open-charm analysis	
	Function	Constraint
Signal	Double Gaussian	Gaussian
Cabibbo-supp bkg.	Johnson	Gaussian
Partially rec. bkg.	Error function	Free
Combinatorial	Exponent	Free
π/K swap bkg.	–	

Channels:

- $B^{\pm} \rightarrow J/\Psi(1S)K^{\pm}$
- $B_s \rightarrow J/\Psi(1S)\phi(\rightarrow KK)$
- $B^0 \rightarrow J/\Psi(1S)K^*(\rightarrow K\pi)$

Measure the relative efficiency-corrected yield R to test the dependency of PFRs on p_T :

- $\mathcal{R}_s = \dfrac{N^{corr}_{B_S^0}}{N^{corr}_{B^{\pm}}}$

- $\mathcal{R}_s^d = \dfrac{N^{corr}_{B_S^0}}{N^{corr}_{B^0}}$

- $f_d/f_u = \dfrac{\mathcal{B}(B^{\pm} \rightarrow J/\Psi(1S)K^{\pm})}{\mathcal{B}(B^0 \rightarrow J/\Psi(1S)K^*(\rightarrow K\pi))} \dfrac{N^{corr}_{B^0}}{N^{corr}_{B^{\pm}}}$
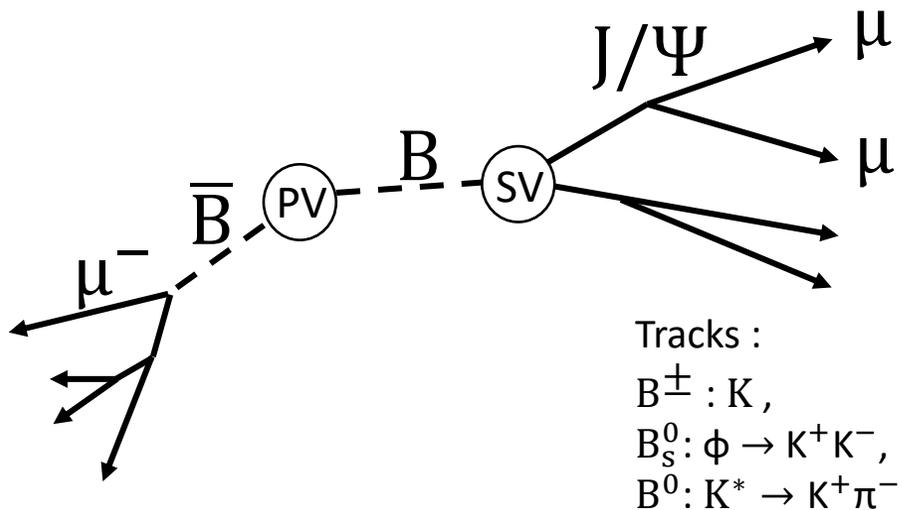
$\mathcal{R}_s$, $\mathcal{R}_s^d$ cannot be directly connected to PFR as $\mathcal{B}(B_s \rightarrow J/\Psi\phi)$ contains f_s/f_u

- Only can determine **a trend in p_T or rapidity**

Conversion from $\mathcal{R}_s$, $\mathcal{R}_s^d$ to f_s/f_u, f_s/f_d is derived using hadronic open-charm channel yields

Selection criteria

Events

- Classified as **tag** or **probe** depending on whether a muon from the B decay of interest fired the corresponding trigger

Muons

- $p_T > \begin{cases} 3.5 & : \quad |\eta| < 1.1 \\ 3.5 + \frac{(1.5\,-3.5)}{(1.5-1.1)} * (|\eta| - 1.1) & : 1.1 < |\eta| < 1.5 \\ 1.5 & : 1.5 < |\eta| < 2.4 \end{cases}$
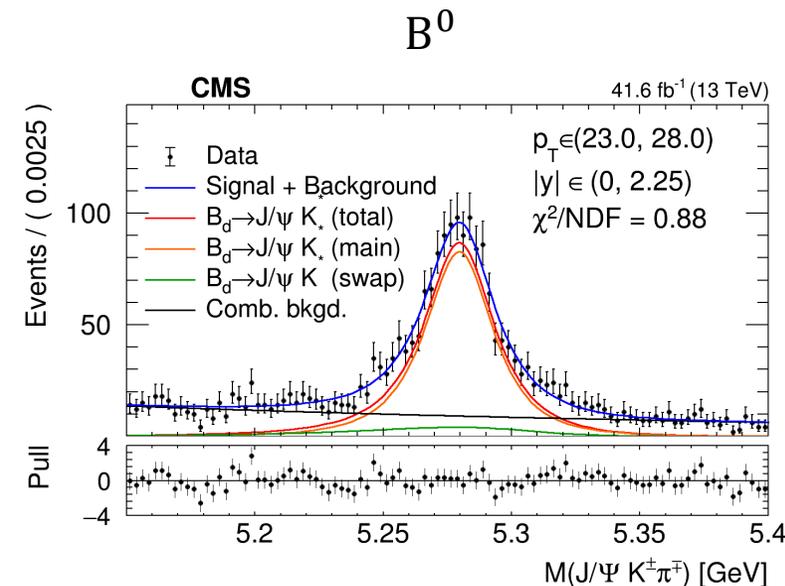
Tracks :
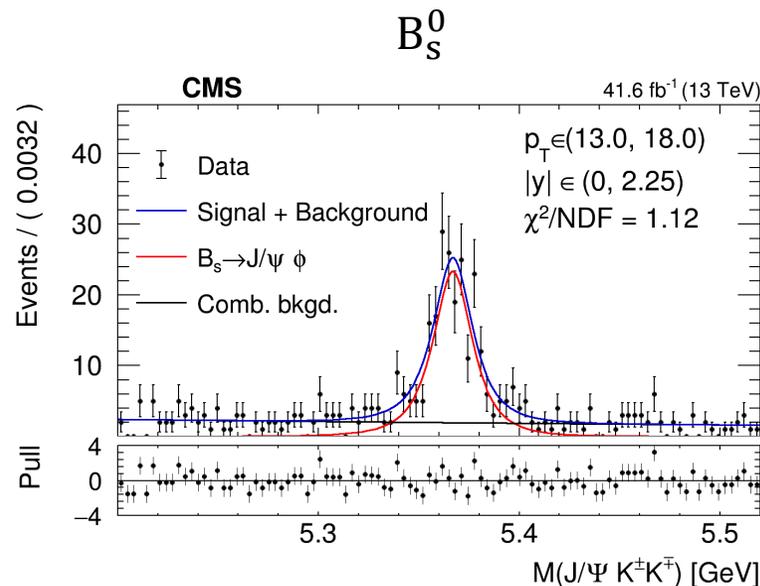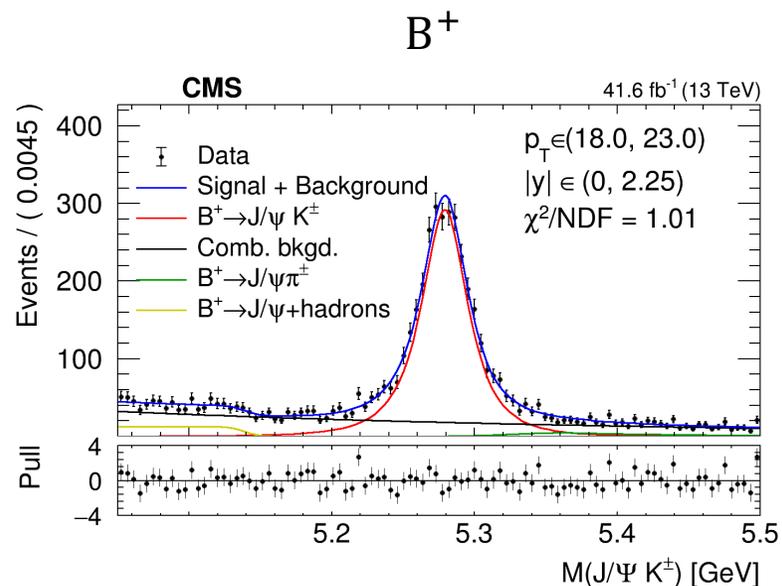$B^\pm : K$,
$B^0_s: \phi \to K^+K^-$,
$B^0: K^* \to K^+\pi^-$

Tracks

- leading p_T $0.85 <$ GeV, subleading p_T $0.6 <$ GeV, $|\eta| < 2.4$.

- For $B^\pm$,only the leading cut is applied

- For K^* in B^0 ,only the combination with the mass closest to the nominal K^* mass

Secondary vertex (B^+ ,B^0_s ,B^0)

- L_{xy} significance > 4.0, Prob(SV) > 0.07, $\cos\alpha$ 2D > 0.997

- J/Ψ mass constraint

Mass windows:

- B^0_s :
    - $|m(K^+K^-) - m(\phi)| < 10$ MeV
    - $|m(K^+\pi^-) - m(K^*(892))| > 50$ MeV
- B^0 :
    - $|m(K^+\pi^-) - m(K^*(892))| < 50$ MeV
    - $|m(K^+K^-) - m(\phi)| > 10$ MeV

B^+ B_s^0 B^0

Signal (including π/K-swap in B^0)

$$\text{PDF(Johnson)} = \frac{\delta}{\lambda\sqrt{2\pi}}\frac{1}{\sqrt{(1+(\frac{x-\eta}{\lambda})^2)}}\exp(-\frac{1}{2}(\gamma + \delta\sinh^{-1}(\frac{x-\eta}{\lambda}))^2)$$

Backgrounds:

Background	Combinatorial	Partially reco.	Cabbibo-supp
$B_s^0 \to J/\psi(\mu^+\mu^-)\phi(1020)(K^+K^-)$	Exponential	-	-
$B^0 \to J/\psi(\mu^+\mu^-)K^{*0}(892)(K^+\pi^-)$	Exponential	-	-
$B^+ \to J/\psi(\mu^+\mu^-)K^+$	Exponential	Error function	Crystall Ball

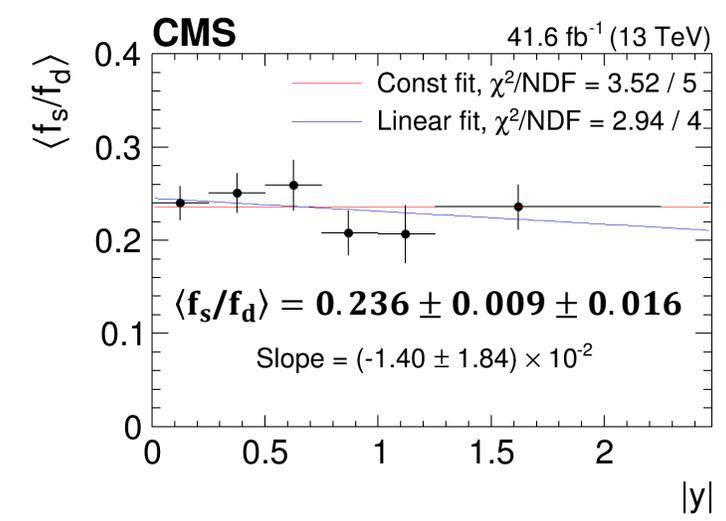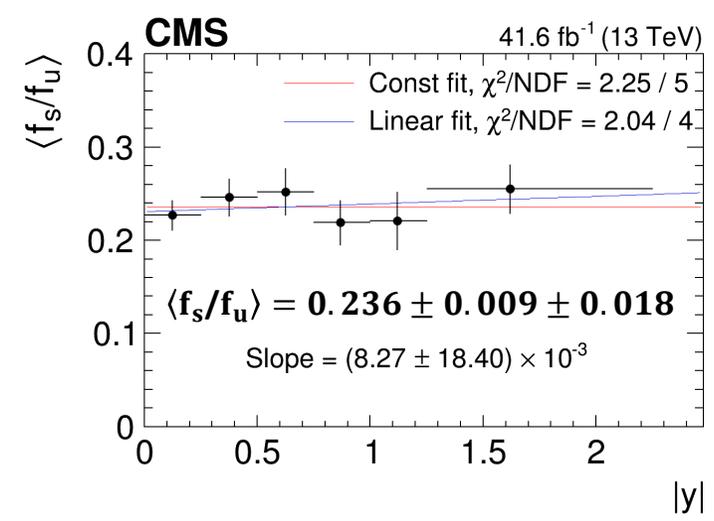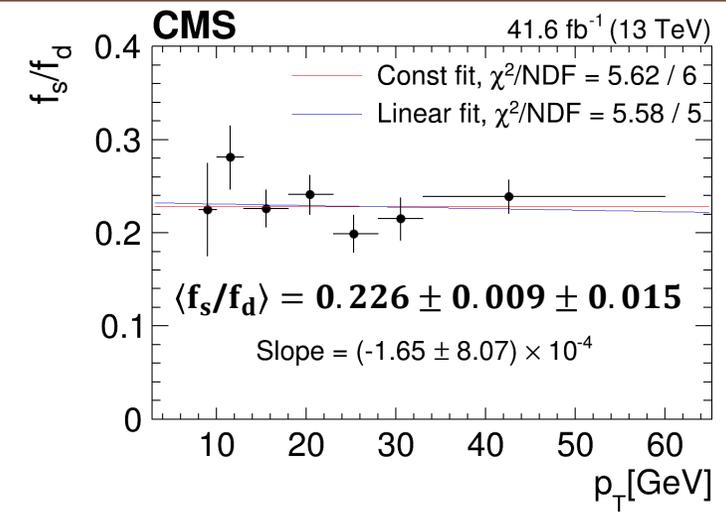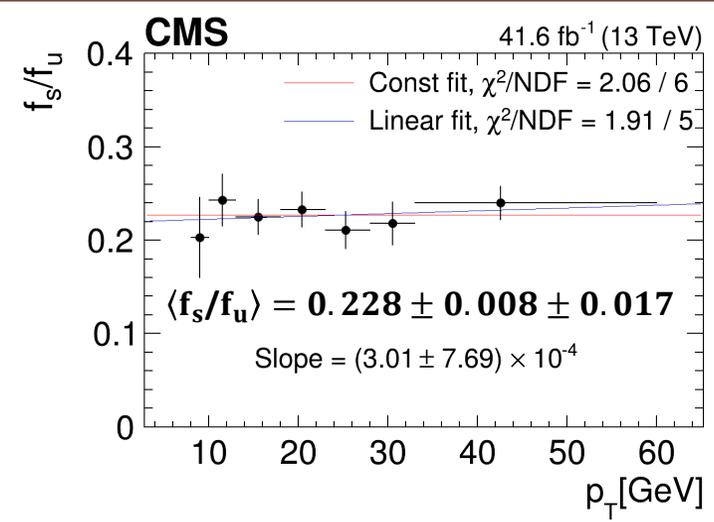|	Charmonium analysis	
Source	Function	Constraint
Signal	Johnson	μ, λ: Free; δ, γ: Fixed
Cabibbo-supp bkg.	Crystal Ball + Gaussian	Fixed
Partially rec. bkg.	Error function	Free
Combinatorial	Exponent	Free
π/K swap (signal)	Johnson	Fixed

Absolute PFR measurement

Determined using Hadronic open-charm decays

It shows little indication of either linear p_T or $|y|$ dependency of the PFR

- $p_T \in [8, 60]$ GeV and $|y| \in [0.0, 2.25]$

$\langle \rangle$ **is added to show that f_s/f_u and f_s/f_d are potentially affected by the p_T dependence**

- Previous CMS & LHCb studies

Plot top-left: f_s/f_u vs p_T[GeV]. CMS, 41.6 fb^{-1} (13 TeV). Const fit, χ^2/NDF = 2.06 / 6; Linear fit, χ^2/NDF = 1.91 / 5. $\langle f_s/f_u \rangle = 0.228 \pm 0.008 \pm 0.017$. Slope = $(3.01 \pm 7.69) \times 10^{-4}$.

Plot top-right: f_s/f_d vs p_T[GeV]. CMS, 41.6 fb^{-1} (13 TeV). Const fit, χ^2/NDF = 5.62 / 6; Linear fit, χ^2/NDF = 5.58 / 5. $\langle f_s/f_d \rangle = 0.226 \pm 0.009 \pm 0.015$. Slope = $(-1.65 \pm 8.07) \times 10^{-4}$.

Plot bottom-left: $\langle f_s/f_u \rangle$ vs $|y|$. CMS, 41.6 fb^{-1} (13 TeV). Const fit, χ^2/NDF = 2.25 / 5; Linear fit, χ^2/NDF = 2.04 / 4. $\langle f_s/f_u \rangle = 0.236 \pm 0.009 \pm 0.018$. Slope = $(8.27 \pm 18.40) \times 10^{-3}$.

Plot bottom-right: $\langle f_s/f_d \rangle$ vs $|y|$. CMS, 41.6 fb^{-1} (13 TeV). Const fit, χ^2/NDF = 3.52 / 5; Linear fit, χ^2/NDF = 2.94 / 4. $\langle f_s/f_d \rangle = 0.236 \pm 0.009 \pm 0.016$. Slope = $(-1.40 \pm 1.84) \times 10^{-2}$.
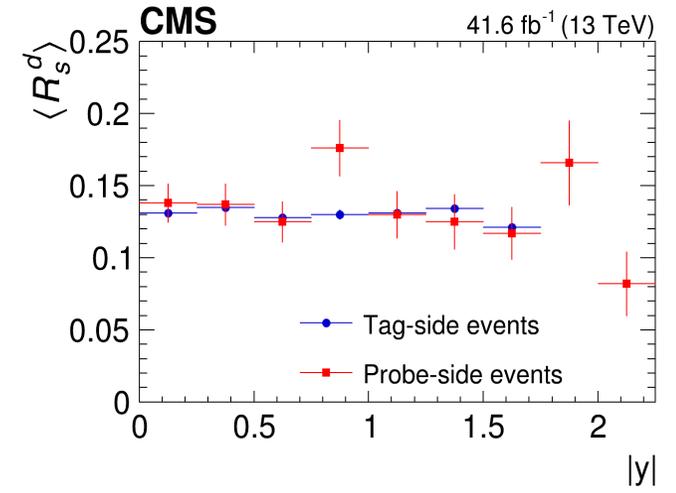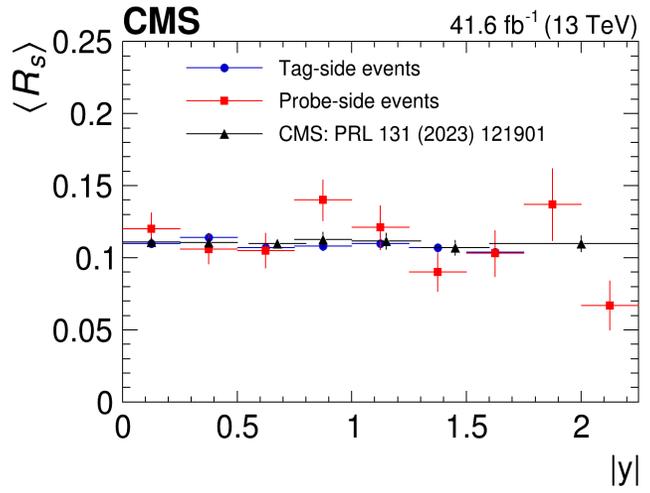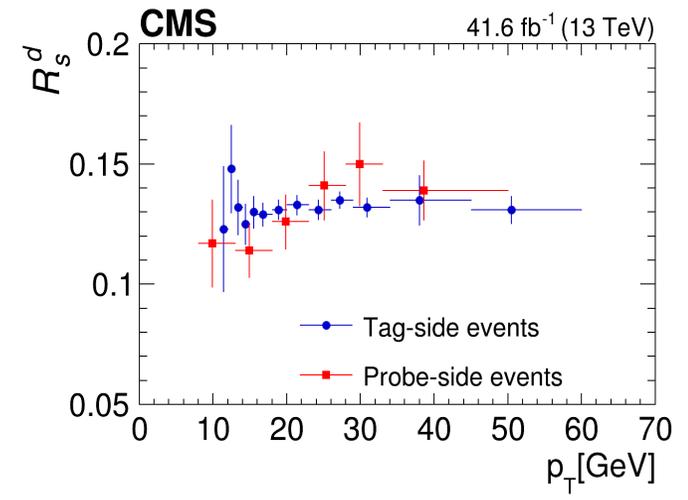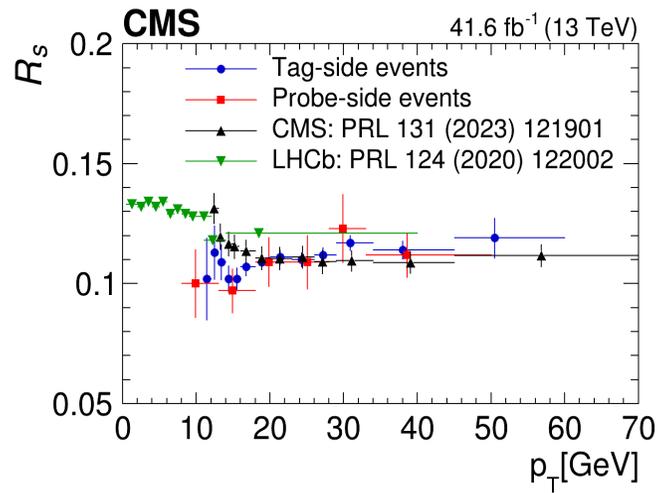
Determined using Charmonium decays

Results from tag and probe-side events are consistent
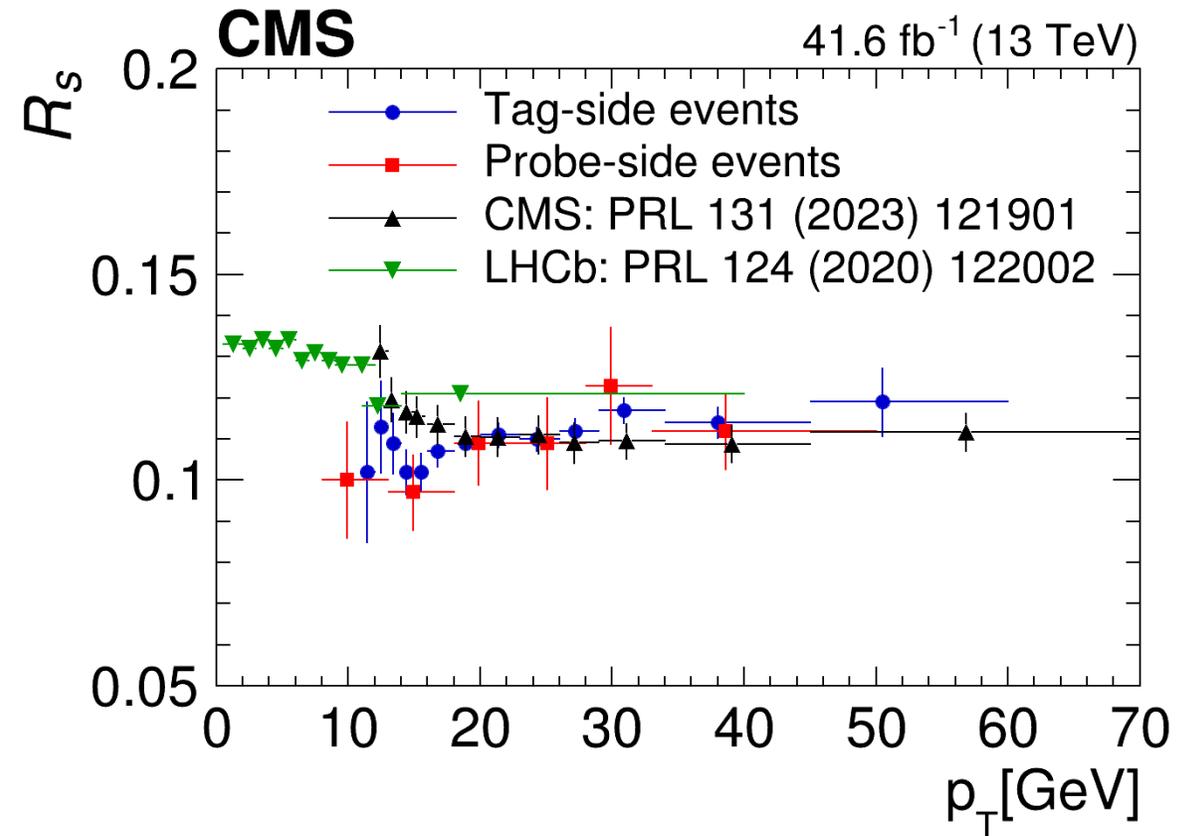
- No rapidity dependence observed

$\langle\ \rangle$ **indicates that $\mathcal{R}_s$ and $\mathcal{R}_s^d$ are potentially affected by the p_T dependence**

- This **does not impact the determination of the trend**
  - **p_T and rapidity independent** within the kinematic region of this study

Comparison with previous measurements

- There is **overlap in data between this and previous CMS study**

- **High p_T ($p_T > 18$ GeV)**
  - All results are consistent
  - Re-confirm the asymptotical flatness in $p_T > 18$ GeV

- **Low p_T ($p_T < 18$ GeV)**
  - vs Previous CMS: 2.1 σ deviation (upper bound)
    - From 12 to 18 GeV
  - vs LHCb: less than 2 σ
  - **Not exclude non-linear p_T dependence** of PFR

f_d/f_u measurement
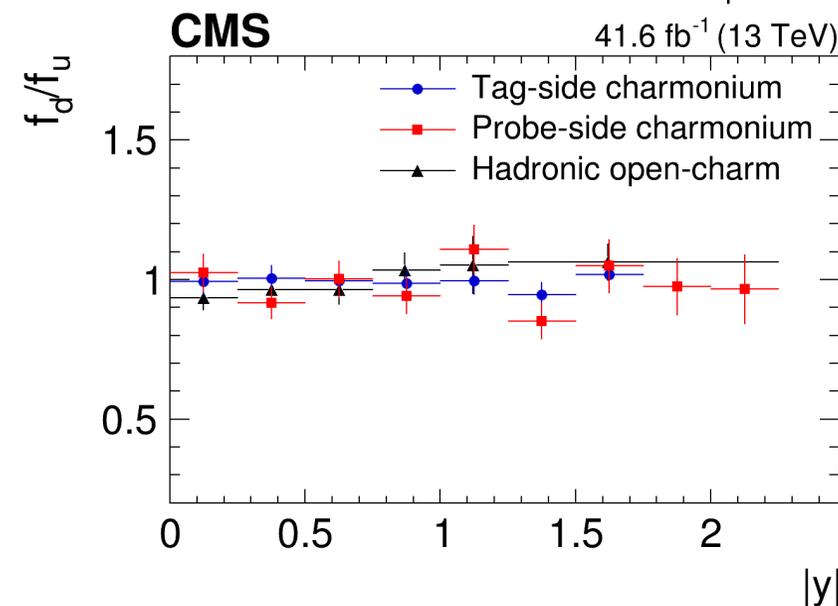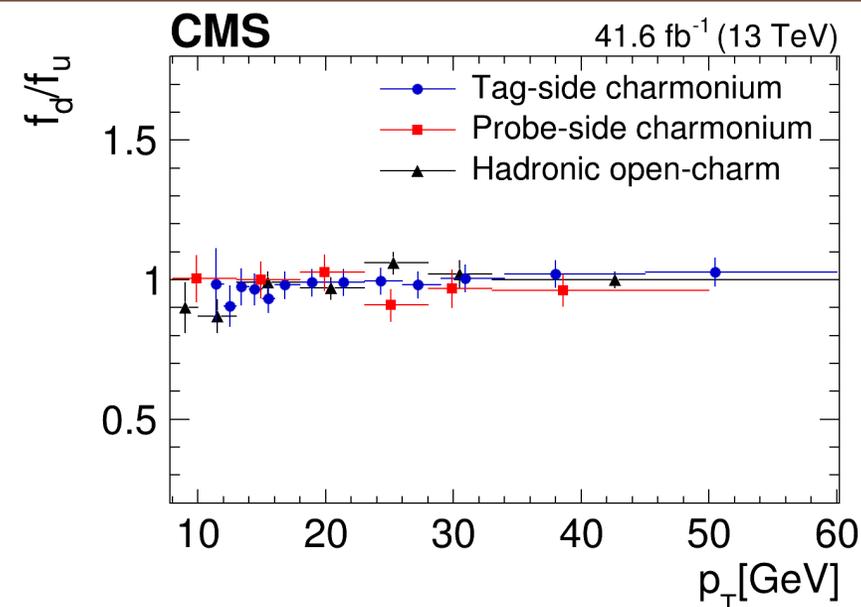
f_d and f_u are generally assumed to be equal

- Good assumption in case of e^+e^- collisions (isospin singlet)
- not necessarily apply in case of **hadron colliders (isospin triplet)**
- $r^{+0} = \frac{\mathcal{B}(Y(4s) \to B^+B^-)}{\mathcal{B}(Y(4s) \to B^0\overline{B^0})} = 1.057 \pm 0.023$ **[PRD 110 (2024) 914997]**

Explicitly measure the f_d/f_u at hadron colliders

- Need to cancel out **all the assumptions on isospin variance** in external inputs
- $B^+ \to \pi^+\overline{D}^0(K^+\pi^-)$, $B^0 \to \pi^+D^-(K^+\pi^-\pi^-)$, $B^\pm \to J/\Psi(1S)K^\pm$
    - $r^{+0} = 1.058 \pm 0.024$
- $B^0 \to J/\Psi(1S)K^*(\to K\pi)$
    - $r^{+0} = 1$

The f_d/f_u measurement

- f_d/f_u (hadronic) = 0.967 ± 0.014 (stat) ± 0.063 (syst)
- f_d/f_u (charmonium, tag) = 0.984 ± 0.005 (stat) ± 0.055 (syst)
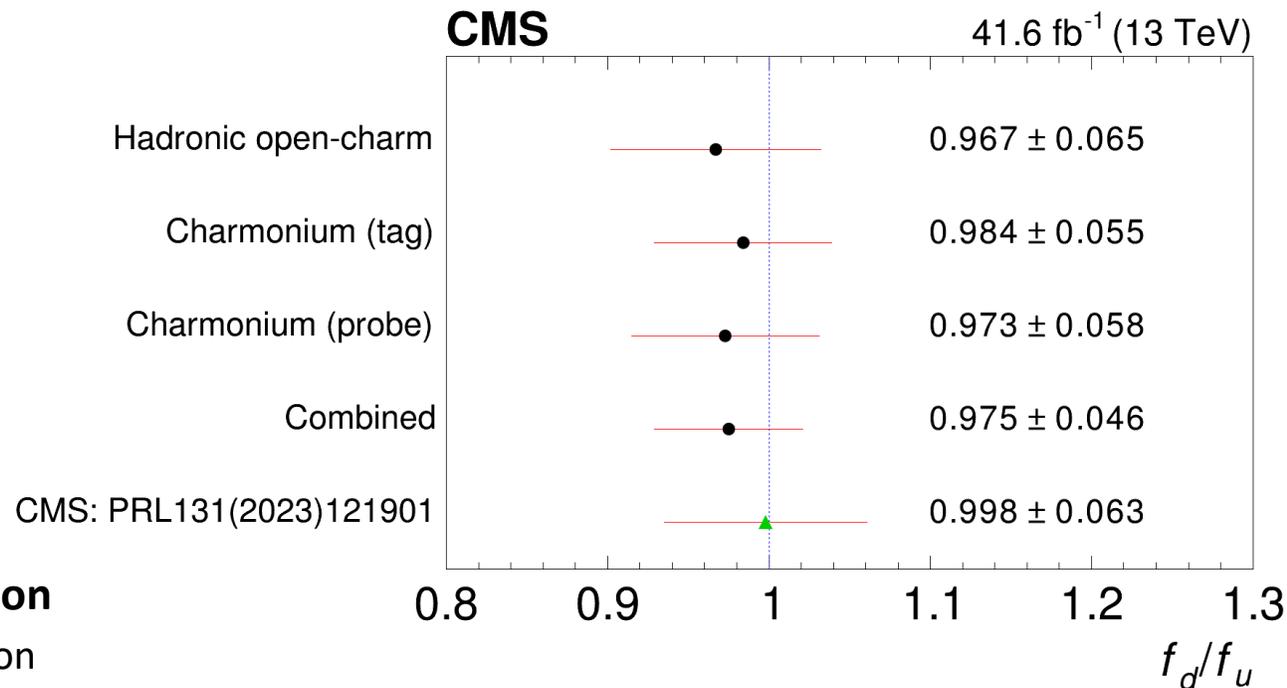- f_d/f_u (charmonium, probe) = 0.973 ± 0.007 (stat) ± 0.058 (syst)

Combined fit on hadronic open-charm and charmonium

- Correlations within each analysis
  - Branching fractions
  - BDT efficiency
- Correlation between two analysis
  - Tracking efficiency
  - $r^{+0} = 1.057 \pm 0.023$
- $\mathbf{f_d/f_u = 0.975 \pm 0.046}$

CMS   41.6 fb^{-1} (13 TeV)

Hadronic open-charm	0.967 ± 0.065
Charmonium (tag)	0.984 ± 0.055
Charmonium (probe)	0.973 ± 0.058
Combined	0.975 ± 0.046
CMS: PRL131(2023)121901	0.998 ± 0.063

0.8   0.9   1   1.1   1.2   1.3

f_d/f_u

The f_d/f_u value is consistent with unity within a 4.6% precision

- Supporting isospin invariance in B meson production at hadron colliders
- Previous CMS: $\mathbf{f_d/f_u = 0.998 \pm 0.063}$

Connection from $B \to J/\Psi$ to $B \to D$ is determined with a precision comparable with PDG

- p_T dependence effect is canceled out in the double ratio, c_{sd} and c_{su}

It gives the conversion factor from $\mathcal{R}$ to f_s/f_d

$c_{sd} := f_s/f_d \text{ (open-charm)}/\mathcal{R}_s^d \text{ (charmonium)}$

$$= \Phi_{PS} \cdot |\frac{V_{us}}{V_{ud}}|^2 \cdot (\frac{f_K}{f_\pi})^2 \cdot \frac{\tau_{B^0}}{\tau_{B_s^0}} \cdot \frac{1}{N_a N_F} \cdot \frac{\mathcal{B}(B^0 \to \pi^+ D^-)}{\mathcal{B}(B^0 \to K^+ D^-)}$$

$$\cdot \frac{\mathcal{B}(D^- \to K^+\pi^-\pi^-)}{\mathcal{B}(D_s^- \to \pi^-\phi)} \cdot \frac{N_{corr}(B_s^0 \to \pi^+ D_s^-)}{N_{corr}(B_s^0 \to J/\psi(1S)\phi)} \cdot \frac{N_{corr}(B^0 \to J/\psi(1S)K^*(892))}{N_{corr}(B^0 \to \pi^+ D^-)}$$

$$= 1.684 \pm 0.097 \pm 0.107 = 1.684 \pm 0.144$$
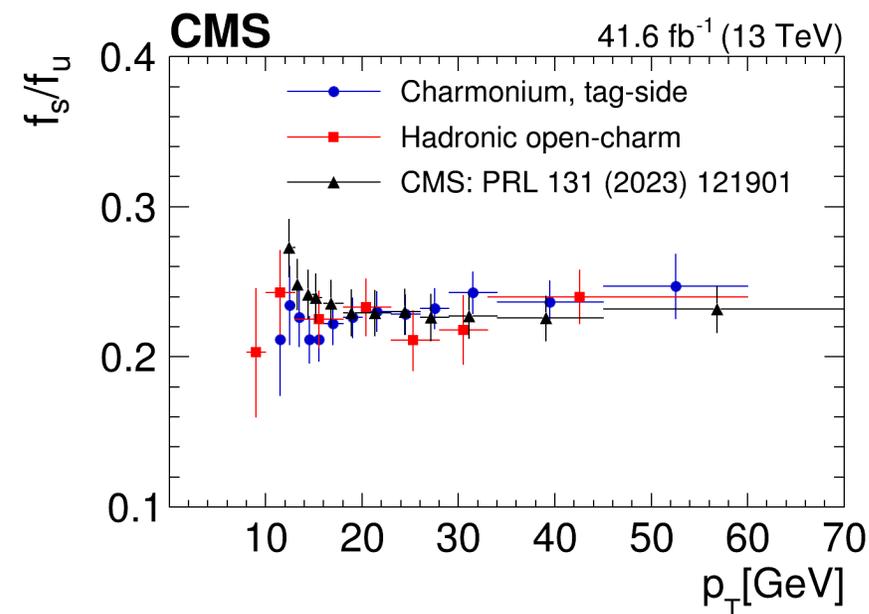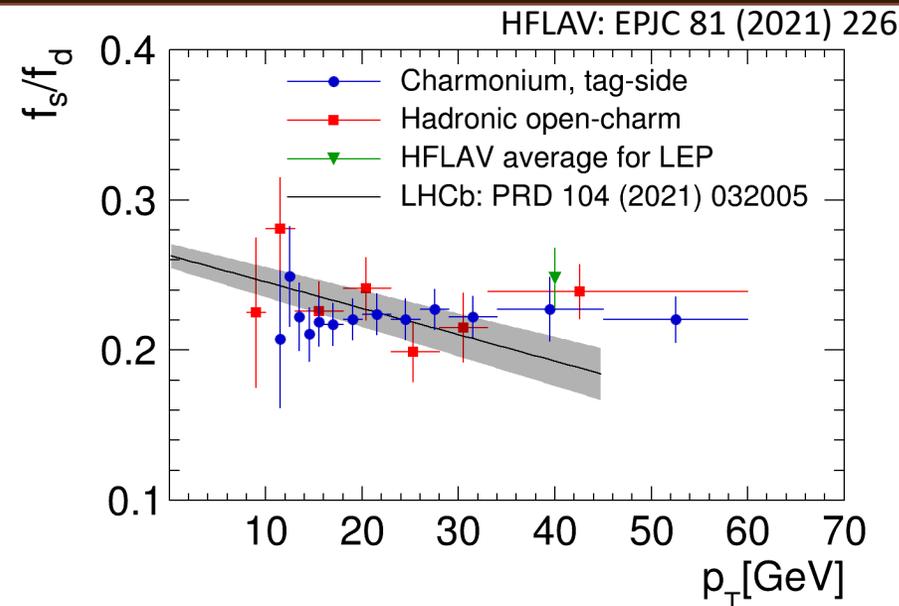
$c_{su} := f_s/f_u \text{ (open-charm)}/\mathcal{R}_s \text{ (charmonium)}$

$$= \Phi_{PS} \cdot |\frac{V_{us}}{V_{ud}}|^2 \cdot (\frac{f_K}{f_\pi})^2 \cdot \frac{\tau_{B^0}}{\tau_{B_s^0}} \cdot \frac{1}{N_a N_F} \cdot \frac{\mathcal{B}(B^\pm \to \pi^+ D^0)}{\mathcal{B}(B^0 \to K^+ D^-)}$$

$$\cdot \frac{\mathcal{B}(D^0 \to K^+\pi^-)}{\mathcal{B}(D_s^- \to \pi^-\phi)} \cdot \frac{N_{corr}(B^\pm \to \pi^\pm D^0)}{N_{corr}(B_s^0 \to J/\psi(1S)\phi)} \frac{N_{corr}(B^\pm \to J/\psi(1S)K^\pm)}{N_{corr}(B^\pm \to \pi^+ D^0)}$$

$$= 2.075 \pm 0.115 \pm 0.153 = 2.075 \pm 0.191$$

The relative PFR measurement in charmonium channels is converted into the absolute PFR

The LHCb trend and all CMS measurements are consistent in low p_T

- The p_T dependence at low p_T still holds
  - f_s/f_d at LHCb : 0.2539 ± 0.0079 (13 TeV)
    - $p_T \in [1.5, 40]$ GeV

- The p_T dependence **flatten out in high p_T** ($p_T > 18$ GeV)
  - Consistent with f_s/f_d at LEP : 0.249 ± 0.023

HFLAV: EPJC 81 (2021) 226

Summary

Absolute normalization of B Production fraction ratio is first measured in CMS

- From probe-side events of 2018 B parking data sample (41.6 fb^{-1})

The test of $\mathbf{p_T}$ dependency of the PFRs is performed

- Re-confirmed that there is **no global linear $\mathbf{p_T}$ trend of PFR**
  - Flat over $p_T > 18$ GeV
- No statistically significant dependence on B meson kinematics
  - Consistent with LHCb trend and the previous CMS measurement in low p_T
  - **Non-linear $\mathbf{p_T}$ dependence of PFR** still holds

The $\mathbf{f_d/f_u}$ measurement is performed in proton-proton collisions

- The f_d/f_u value is consistent with **unity within a 4.6% precision**

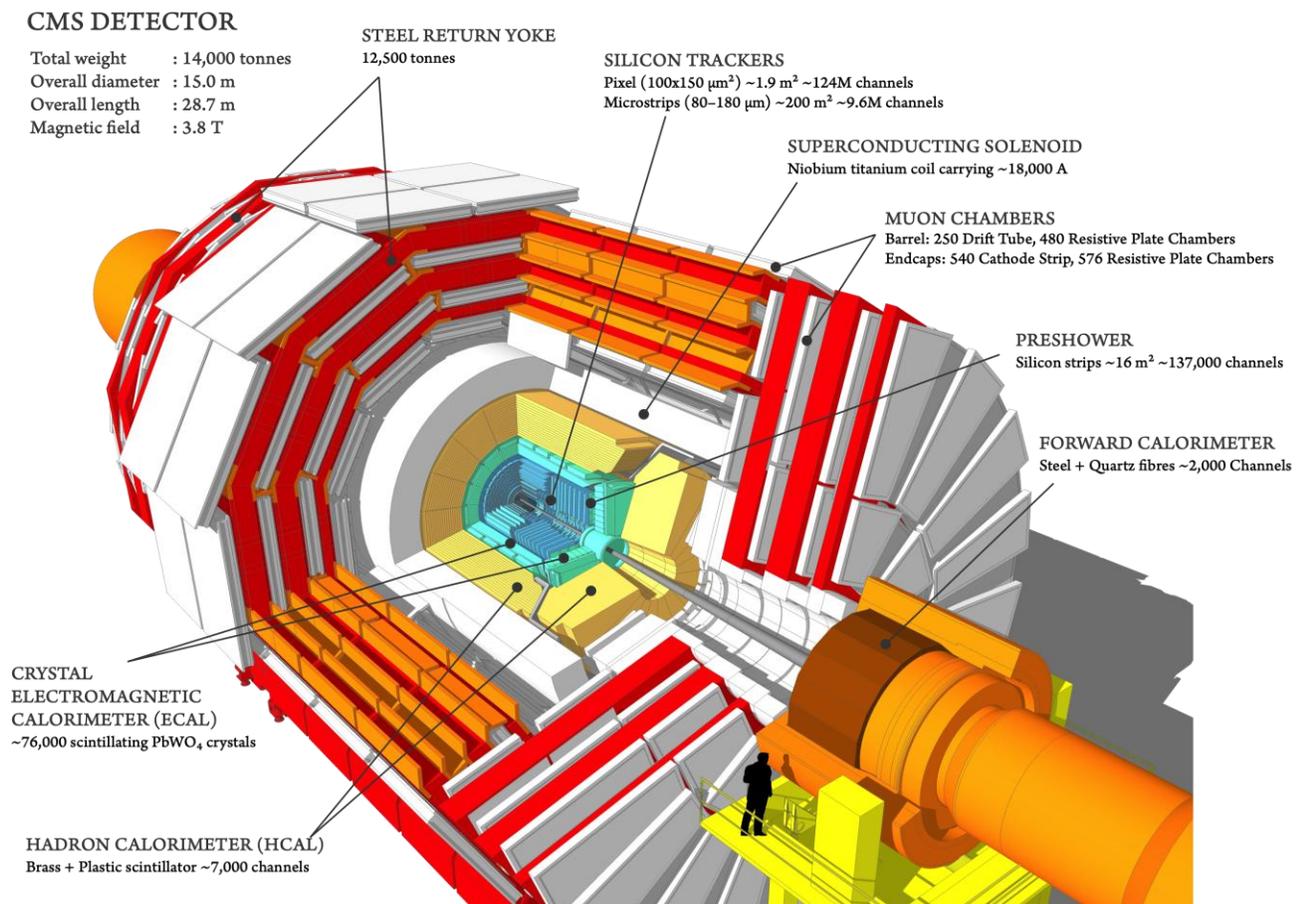**The conversion factor from the efficiency-corrected yield ratio $\mathcal{R}$ to PFR is derived for the first time**

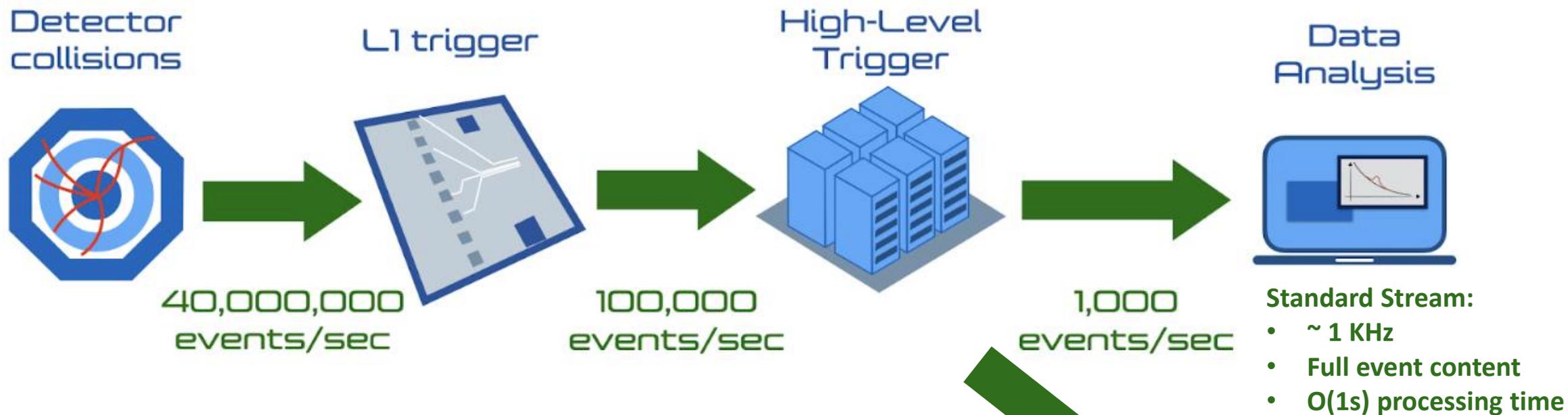- Variables **independent of $\mathbf{p_T}$-dependence of PFRs**

Back up

Compact Muon Solenoid (CMS) is one of general-purpose detector at LHC

- **Not originally designed for flavor physics** in mind
- But **can be competitive in several measurements** due to…
- ➢ Excellent solid angle coverage

- ➢ State-of-the-art all-silicon tracker
  - Provides high-precision vertex reconstruction

- ➢ Strong magnetic field (3.8 T)
  - Enables precise momentum measurements

- ➢ Redundant detector systems
  - Ensures reliable muon identification

CMS DETECTOR

Total weight	: 14,000 tonnes
Overall diameter	: 15.0 m
Overall length	: 28.7 m
Magnetic field	: 3.8 T

STEEL RETURN YOKE
12,500 tonnes

SILICON TRACKERS
Pixel (100x150 μm²) ~1.9 m² ~124M channels
Microstrips (80–180 μm) ~200 m² ~9.6M channels

SUPERCONDUCTING SOLENOID
Niobium titanium coil carrying ~18,000 A

MUON CHAMBERS
Barrel: 250 Drift Tube, 480 Resistive Plate Chambers
Endcaps: 540 Cathode Strip, 576 Resistive Plate Chambers

PRESHOWER
Silicon strips ~16 m² ~137,000 channels

FORWARD CALORIMETER
Steel + Quartz fibres ~2,000 Channels

CRYSTAL ELECTROMAGNETIC CALORIMETER (ECAL)
~76,000 scintillating PbWO₄ crystals

HADRON CALORIMETER (HCAL)
Brass + Plastic scintillator ~7,000 channels

Data parking at CMS

Detector collisions → L1 trigger → High-Level Trigger → Data Analysis

40,000,000 events/sec → 100,000 events/sec → 1,000 events/sec

Standard Stream:
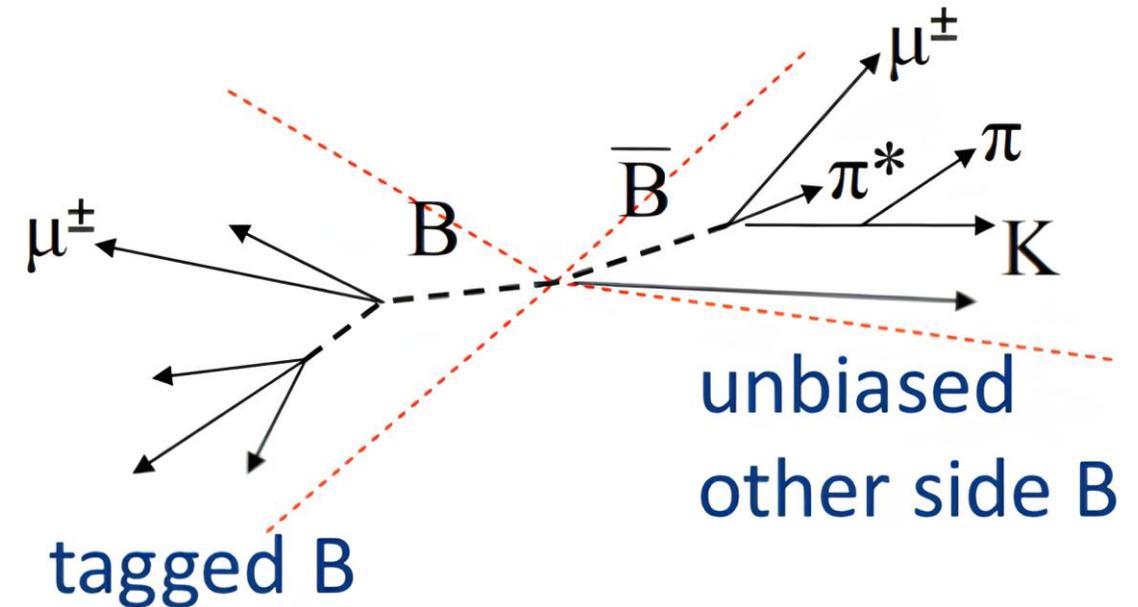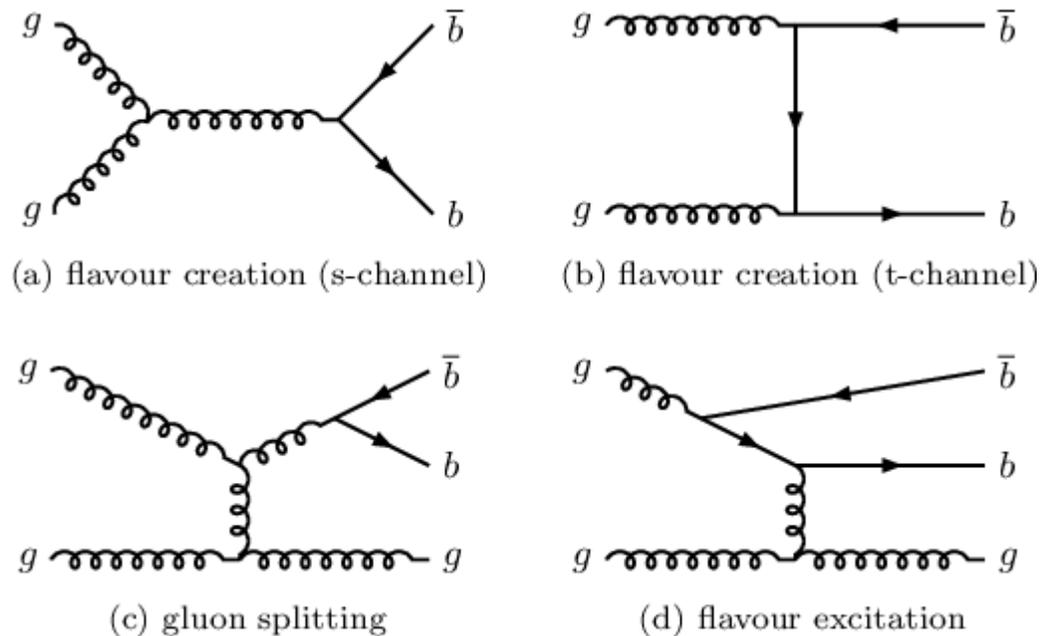- ~ 1 KHz
- Full event content
- O(1s) processing time

CMS introduced a new trigger strategy, "data parking," for B physics studies
- The main **computational bottleneck** occurs after HLT during data processing
- Decision time at different trigger levels:
  - L1: ~ 3.2 μs
  - HLT: ~ 300 ms
  - **Prompt reconstruction: ~ O(1s)**
- Data parking stores full event content after for later reconstruction

Parking Stream:
- ~ 3 KHz
- Full event content
- Reconstruct later

PoS LHCP2019, 210 (2019)

(a) flavour creation (s-channel)

(b) flavour creation (t-channel)

(c) gluon splitting

(d) flavour excitation

Bottom quarks are always produced in pair ($b\bar{b}$)

- Most originate from flavor creation (gg → $b\bar{b}$) and **back-to-back**

B hadrons travel before decaying, producing displaced secondary vertices

- Triggers select one single displaced muon from one B hadron (**tag side**)
- The opposite B hadron (**probe side**) remains unbiased

Data

B parking dataset :

- **Run 2 pre-UL MINIAOD** samples are used
- /ParkingBPHxx/Run2018yy-05May2019-v1/MINIAOD
- xx=1-6, yy=A,B,C,D

Trigger	Lumi column ($10^{34} cm^{-2} s^{-1}$)	Integrated Luminosity (fb^{-1})
HLT_Mu12_IP6	0.9	34.7
HLT_Mu9_IP6	1.3	33.6
HLT_Mu9_IP5	1.5	20.9
HLT_Mu7_IP4	1.7	6.94

- Combination of all **4 Single displaced muon triggers**
  - These triggers are **"nested"**, with successively lower thresholds towards end of runs

MC samples:

- Single muon filter: $p_T(\mu) > 5$ GeV, $|\eta| < 2.5$
- 3 central MC samples per channel:
    1) Require B hadron decay ($B \rightarrow \pi D$) with the muon filter
    2) Require B hadron decay ($B \rightarrow \pi D$) without the muon filter (filter efficiency)
    3) Require B hadron decay ($B \rightarrow KD$) with the muon filter (background)

Dataset name	Events
BuToD0BarPi_D0BarToKPi_MuFilter_TuneCP5_13TeV_pythia8-evtgen BsToDsPi_DsToPhiPi_PhiToKK_MuFilter_TuneCP5_13TeV_pythia8-evtgen B0ToDPi_DToKPiPi_MuFilter_TuneCP5_13TeV_pythia8-evtgen	20M
BuToD0BarPi_D0BarToKPi_noMuFilter_TuneCP5_13TeV_pythia8-evtgen BsToDsPi_DsToPhiPi_PhiToKK_noMuFilter_TuneCP5_13TeV_pythia8-evtgen B0ToDPi_DToKPiPi_noMuFilter_TuneCP5_13TeV_pythia8-evtgen	2M
BuToD0BarK_D0BarToKPi_MuFilter_TuneCP5_13TeV_pythia8-evtgen BsToDsK_DsToPhiPi_PhiToKK_MuFilter_TuneCP5_13TeV_pythia8-evtgen B0ToDK_DToKPiPi_MuFilter_TuneCP5_13TeV_pythia8-evtgen	10M

Table 2: List of all simulated samples(privately produced samples).
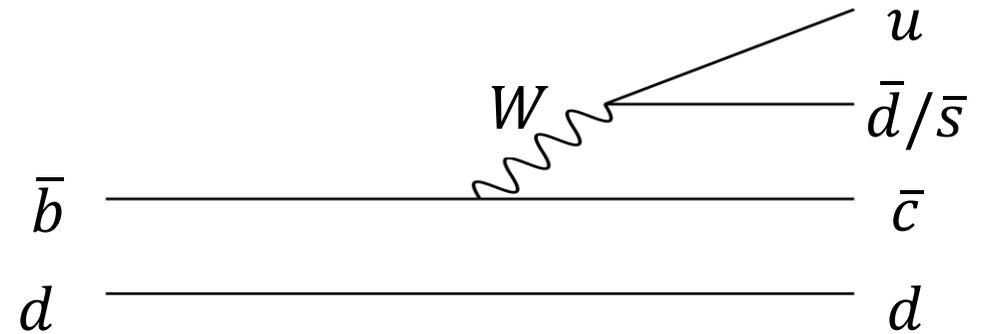
Hadronic Open-charm: PFR measurement

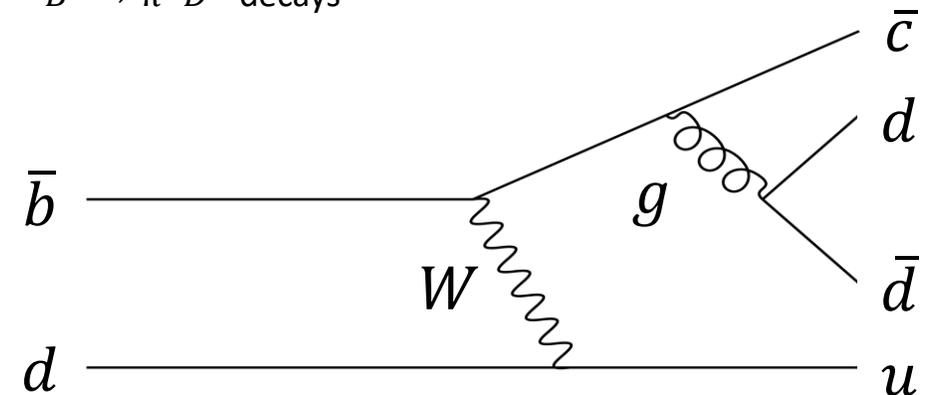The unprecedented size of B parking data sample gives us a room to measure the PFR in rare decay channels

- $\text{Br}(B^+ \to \pi^+ \overline{D}^0(\text{K}^+\pi^-)) = 1.85 \times 10^{-4}$
- $\text{Br}(B_s^0 \to \pi^+ D_s^-(\text{K}^+\text{K}^-\pi^-)) = 1.62 \times 10^{-4}$
- $\text{Br}(B^0 \to \text{K}^+ D^-(\text{K}^+\pi^-\pi^-)) = 1.74 \times 10^{-5}$
- Assuming the selection efficiency of 1-2%, we can have $B^0 \to \text{K}^+ D^-$ events of O(1000)

Why $B^0 \to \text{K}^+ D^-$, not $B^0 \to \pi^+ D^-$?

- $B^0 \to \text{K}^+ D^-$: Double-Cabibbo-suppressed
- $B^0 \to \pi^+ D^-$: Single-Cabibbo-suppressed
- However, because both $\bar{d}$ and d in the final state of $B^0 \to \pi^+ D^-$ decay, there's a subleading annihilation diagram contributing to large uncertainties due to its endpoint divergence [https://arxiv.org/abs/2007.10338]
- $B^0 \to \text{K}^+ D^-$ has more theoretically clean prediction

(a) Leading Cabibbo suppressed diagram of $B^0 \to \text{K}^+ D^-$/ $B^0 \to \pi^+ D^-$ decays

(b) Subleading annihilation diagram of $B^0 \to \pi^+ D^-$

Hadronic Open-charm: External inputs

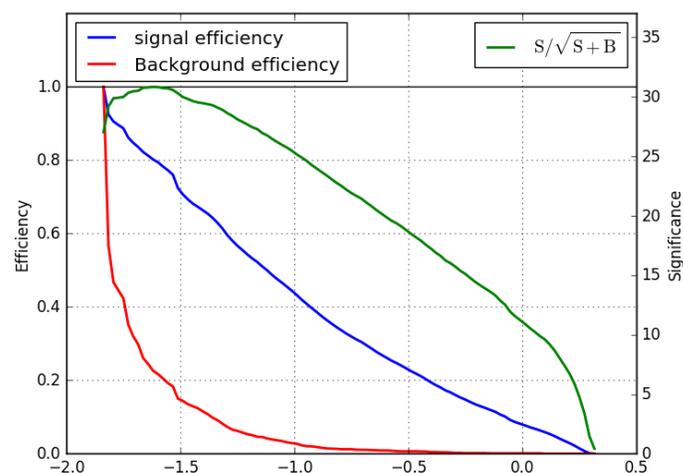| Input variable	Value	Reference
Φ_{PS}	1.02788 ± 0.00014	PDG [8]; Ref. [32], Eq. (7)
$\dfrac{|V_{us}|}{|V_{ud}|}\dfrac{f_K}{f_\pi}$	0.27683 ± 0.00035	Ref. [33], Eq. (107)
$\dfrac{\tau_{B^0}}{\tau_{B^0_s}}$	1.0017 ± 0.0034	HFLAV [11]
$\dfrac{1}{N_a}$	$1.0048^{+0.0046}_{-0.0022}$	Ref. [32], Eq. (20)
$\dfrac{1}{N_F}$	1.002 ± 0.042	Ref. [32], Eq. (16)
$\dfrac{\mathcal{B}(B^0 \to \pi^+ D^-)}{\mathcal{B}(B^0 \to K^+ D^-)}$	0.0819 ± 0.0020	PDG [8]
$\mathcal{B}(D^- \to K^+ \pi^- \pi^-)$	0.0938 ± 0.0016	PDG [8]
$\mathcal{B}(D^-_s \to \pi^- \phi)\mathcal{B}(\phi \to K^+ K^-)$	0.0221 ± 0.0006	PDG [8]
$\mathcal{B}(B^+ \to \pi^+ \overline{D}^0)$	$(4.61 \pm 0.10) \times 10^{-3}$	PDG [8]
$\mathcal{B}(B^0 \to \pi^+ D^-)$	$(2.51 \pm 0.08) \times 10^{-3}$	PDG [8]
$\mathcal{B}(D^0 \to K^- \pi^+)$	0.03947 ± 0.00030	PDG [8]

BDT is trained for the further optimization of $S/\sqrt{S+B}$

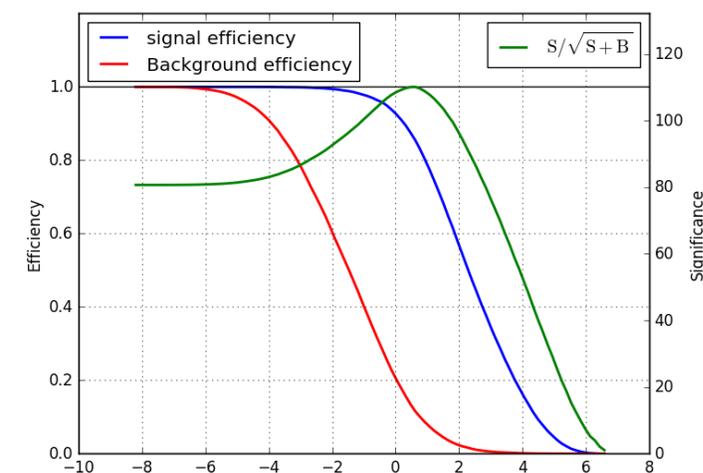- MC samples are weighted by the yields extracted after the pre-selection

Only the right sideband, dominated by combinatorial background is considered

BDT threshold is chosen to maximize the $S/\sqrt{S+B}$

Channel	Signal region	Sideband
B^+	$(5.20, 5.35)$ GeV	$(5.40, 5.55)$ GeV
B_s^0	$(5.30, 5.45)$ GeV	$(5.50, 5.65)$ GeV
B^0	$(5.20, 5.35)$ GeV	$(5.40, 5.55)$ GeV

Variable	Description
trkN_DCASig	Significance of the closest approach of each track to the primary vertex. N = 1, 2, 3 for B^+, and N = 1, 2, 3, 4 for B_s^0, B^0.
BCand_cos2D	cosine of the angle between $\vec{L}_{xy}$(SV) and p_T(B)
BCand_l_xy_sig	transverse flight distance between the secondary vertex and the primary vertex.
BCand_svprob	χ^2 probability of the secondary vertex.
DCand_l_xy_sig	transverse flight distance between the secondary vertex and the primary vertex.
DCand_svprob	χ^2 probability of the tertiary vertex.
DCand_mass	invariant mass of D meson candidate before kinematic fitting.
KKMass	invariant mass of $\phi(\to K^+K^-)$ candidate before kinematic fitting. Only given in B_s^0 channel.

PRD 83 052001
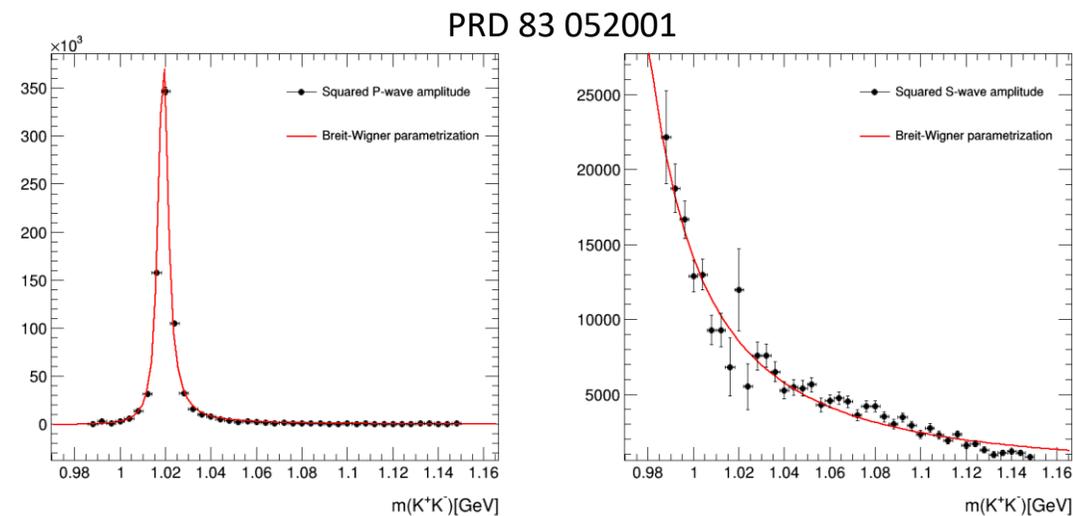
$B_s^0 \to \pi^+ D_s^- (\pi^- \varphi(K^+ K^-))$ **reconstruction**

- **Background from $B^0 \to \pi^+ D^- (K^+ \pi^- \pi^-)$ is rejected** by the narrow φ mass window (10 MeV)

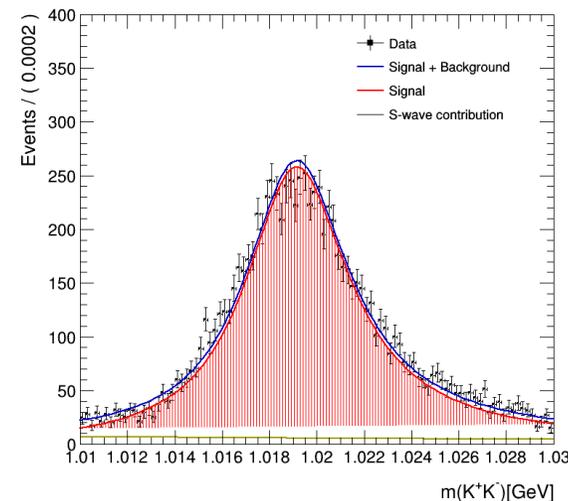**Non-φ resonant background from D_s decay ($\mathcal{S}$-wave) in the mass window need to be subtracted**

- Well investigated in the **BABAR's Dalitz analysis [PRD 83 052001]**
- $\mathcal{S}$-wave/($\mathcal{S}$-wave + $\mathcal{P}$-wave) in 1019.456 $\pm$ 10 MeV of m(K$^+$K$^-$)
  - **5.58 $\pm$ 1.03 %** in this analysis
  - **5.6 $\pm$ 0.9 %** in BaBar's Dalitz analysis

$\mathcal{S}$-wave contribution subtracted using sPlot technique

$\mathcal{P}$-wave parameterization
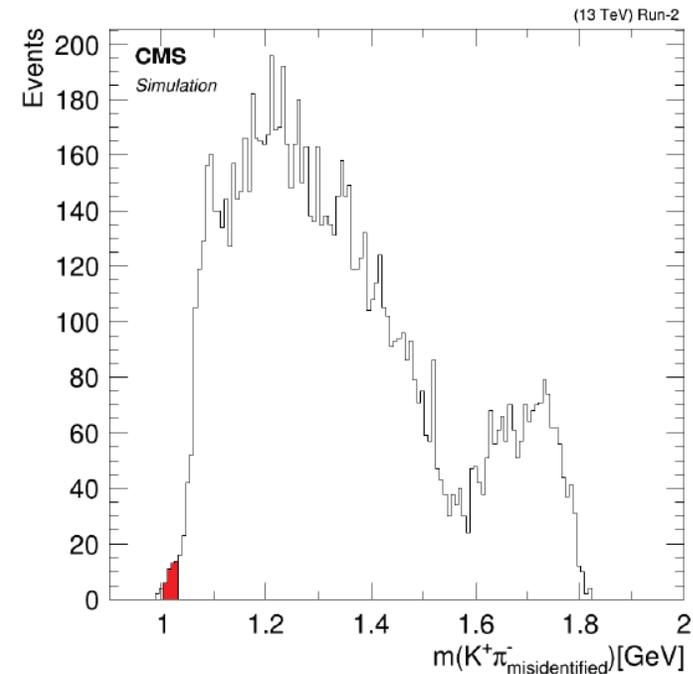

$\mathcal{S}$-wave parameterization

Fitted m(K$^+$K$^-$) distribution in data

(a) The invariant mass distribution of K^+K^- in $B_s^0 \to \pi^+ D_s^- (\to \pi^- \phi(\to K^+K^-))$

(b) The invariant mass distribution of $K^+\pi^-$ with π^- assigned with kaon mass in $B^0 \to \pi^+ D^- (\to K^+ \pi^- \pi^-)$

Figure 1: The performance of ϕ mass window is tested with two simulated samples, $B_s^0 \to \pi^+ D_s^- (\to \pi^- \phi(\to K^+K^-))$ and $B^0 \to \pi^+ D^- (\to K^+ \pi^- \pi^-)$. The red-filled area is ϕ mass window of $|m_\phi - m(K^+K^-)| < 10\,\text{MeV}$. Because the invariant mass distribution of $D^- \to K^+ \pi^- \pi^-$ decays with one π^- assigned with K mass is shifted to the right side, falling in the narrow mass window of D_s^- decay, ϕ mass window is also required to reject B^0-related background in B_s^0 peak. The selection efficiencies are $\epsilon_{\text{sel}} \simeq 83.4\%$ for $B_s^0 \to \pi^+ D_s^-$, and $\epsilon_{\text{sel}} \simeq 0.41\%$ for $B^0 \to \pi^+ D^-$ after the cut-based selection.

Efficiency determination

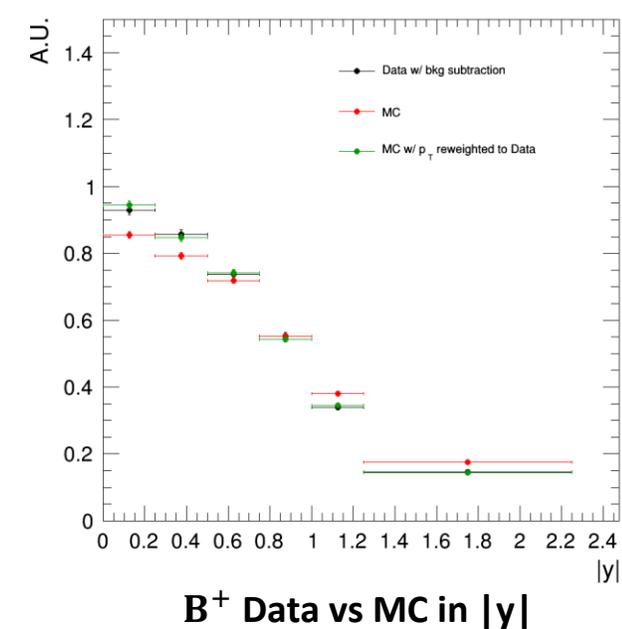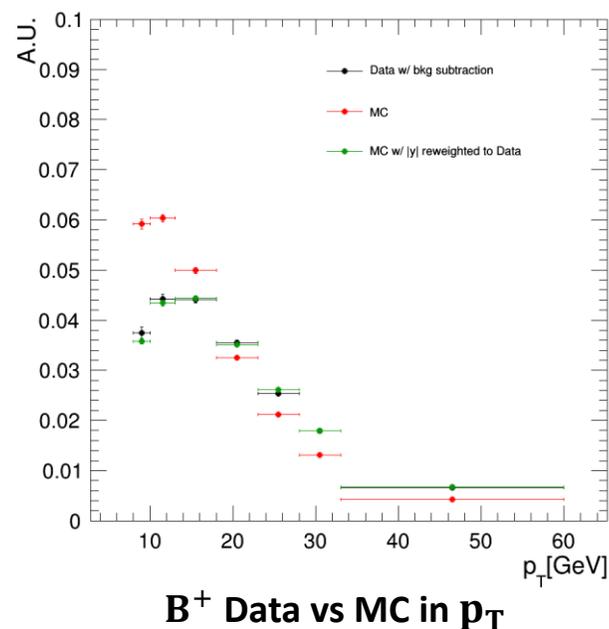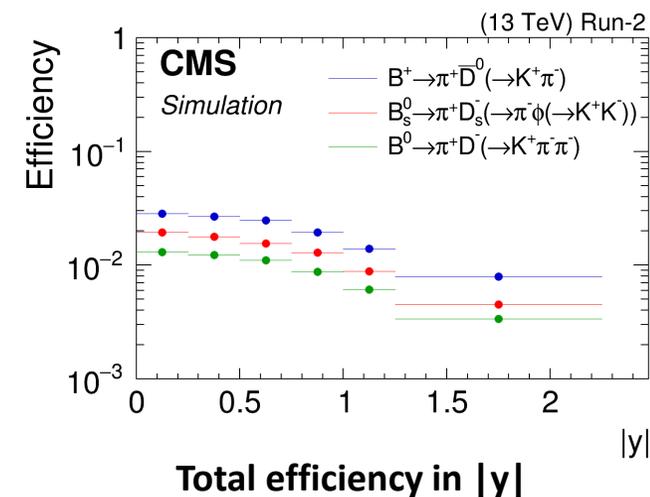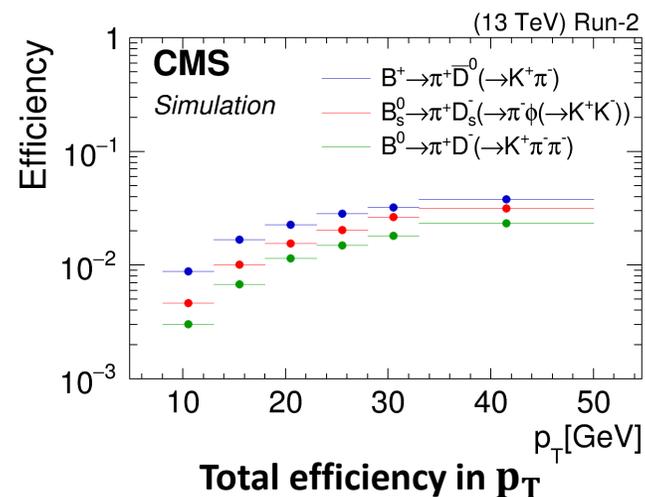**The efficiencies for three channels are determined with single μ filter MC sample**

- Single μ filter which requires a $p_T(\mu) > 6$ GeV to guarantee a trigger muon
- **Filter efficiencies are not included** in final results as these are canceled out in the PFR
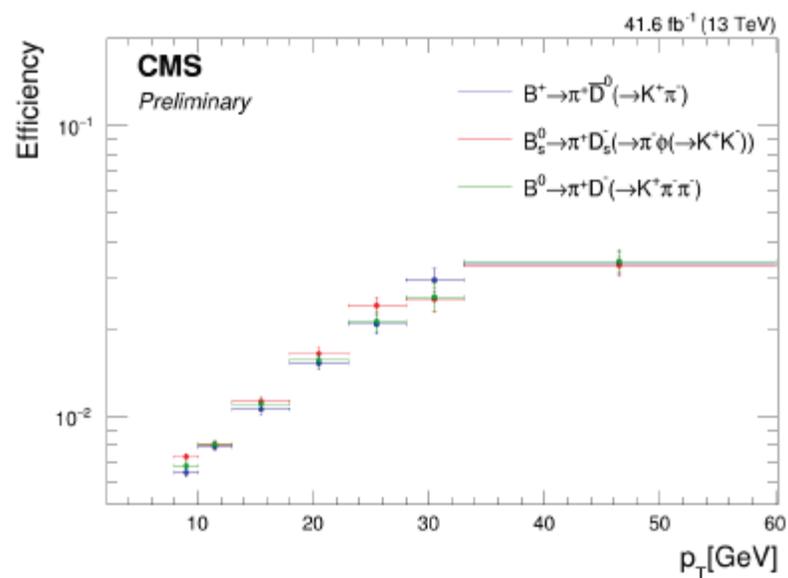
MC samples are reweighted to Data

- To match p_T and rapidity distribution
- The **weights $w_{bin} = \dfrac{Data_{bin}}{MC_{bin}}$** extracted from each channel are parameterized and assigned to each event

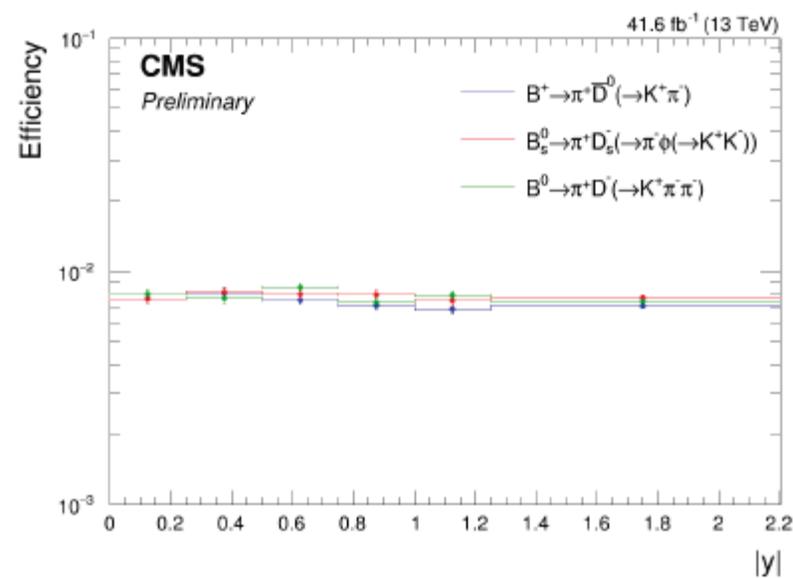**Trigger efficiency is canceled out** in the efficiency ratio

- Probe side is minimally biased by trigger effect
- **Confirmed that trigger SF in data and MC are consistent** in each HLT path

Total efficiency in p_T

Total efficiency in $|y|$

B^+ Data vs MC in p_T
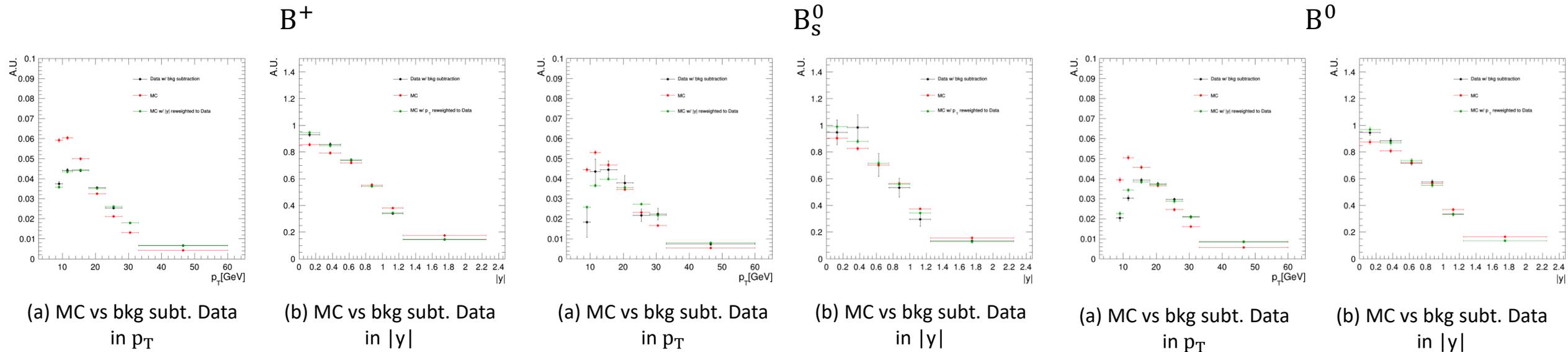

B^+ Data vs MC in $|y|$

(a) p_T bins

(b) $|y|$ bins

Figure 13: Probe filter efficiency in each channel in p_T and $|y|$ bins in $p_T \in [8, 60)$ GeV and $|y| \in [0.0, 2.25)$.
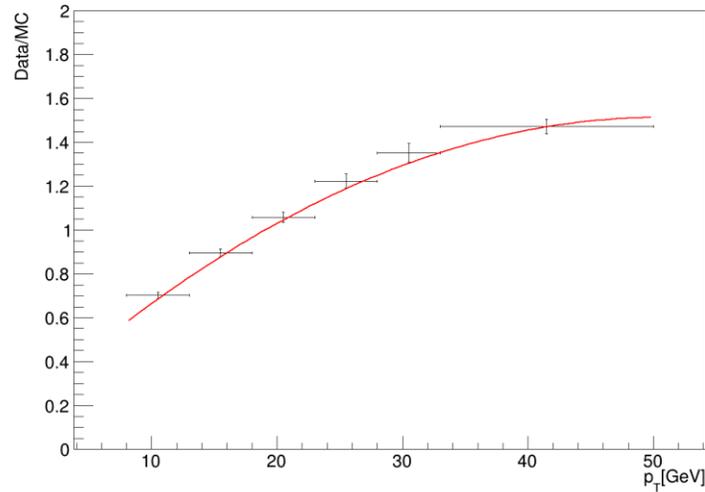
- MC samples are reweighted to bkg subtracted Data

  - $w_{bin} = \dfrac{\text{Data}_{bin}}{\text{MC}_{bin}}$

  - 10 bins in p_T and 7 bins in $|y|$

- The uncertainties in p_T or $|y|$ bins are assigned as the difference in the efficiency between each channel before and after reweighting in $|y|$ or p_T, respectively
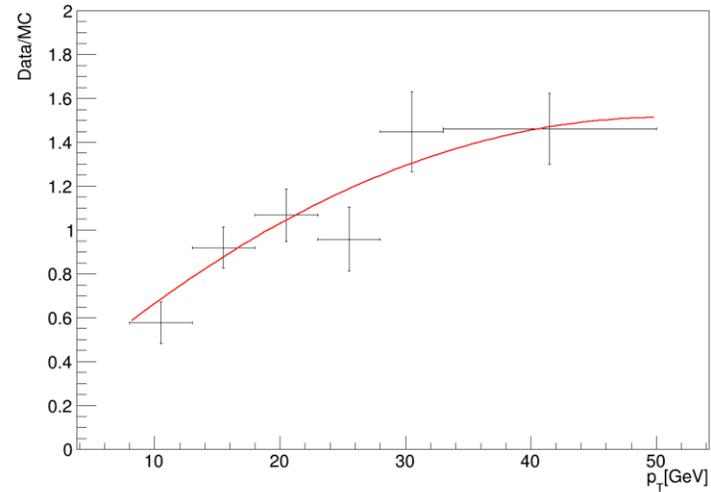
B^+ $\qquad\qquad\qquad\qquad\qquad\qquad$ B_s^0 $\qquad\qquad\qquad\qquad\qquad\qquad$ B^0

(a) MC vs bkg subt. Data in p_T $\qquad$ (b) MC vs bkg subt. Data in $|y|$ $\qquad$ (a) MC vs bkg subt. Data in p_T $\qquad$ (b) MC vs bkg subt. Data in $|y|$ $\qquad$ (a) MC vs bkg subt. Data in p_T $\qquad$ (b) MC vs bkg subt. Data in $|y|$

Hadronic Open-charm: Weights parameterization

W = 0.1940 + 0.0520*[pT] − 0.0005*[pT]^2

- W = 1.1201 -0.1325*[|y|] − 0.02612*[|y|]^2
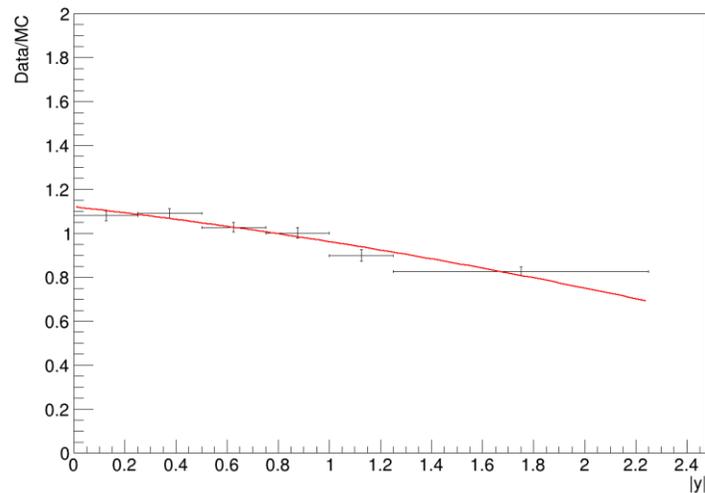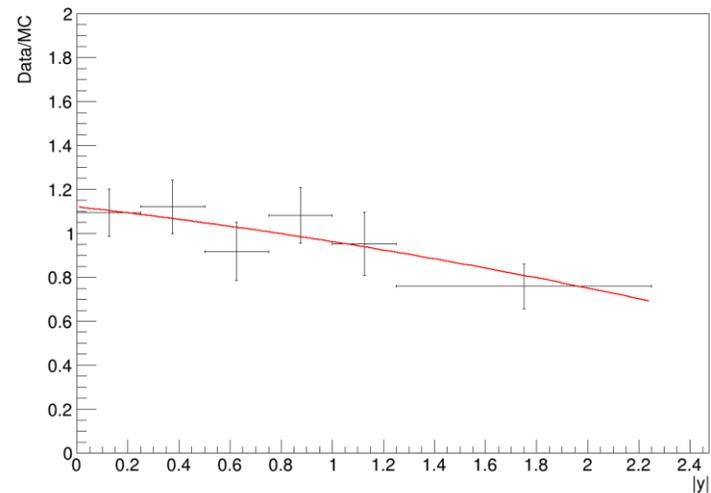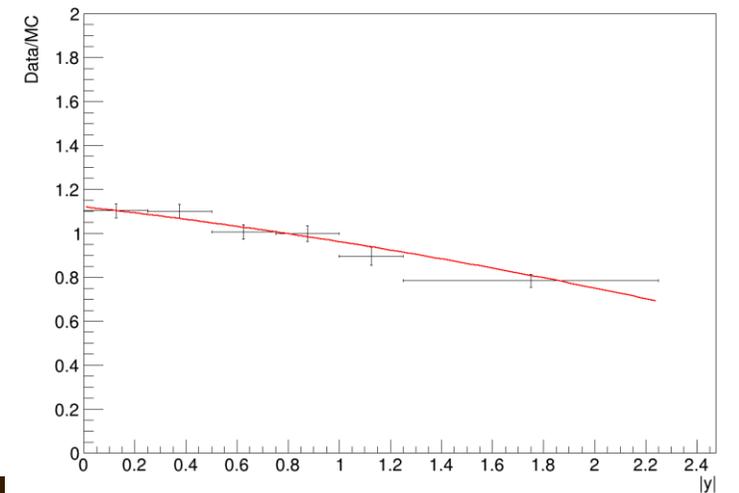
Trigger Efficiency

Trigger efficiency is different between data and MC

- In MC, the lowest threshold trigger (HLT_Mu7_IP4) is always turned on
- In Data, trigger thresholds are gradually decreased toward the end of each fill

Trigger efficiencies should be canceled out in the efficiency ratio (PFR)

Confirmed that trigger efficiencies in data and MC are consistent

- For each HLT path
- Under the condition that **HLT_Mu7_IP4 is on** (as representative)

HLT config

Sara Fiorendi

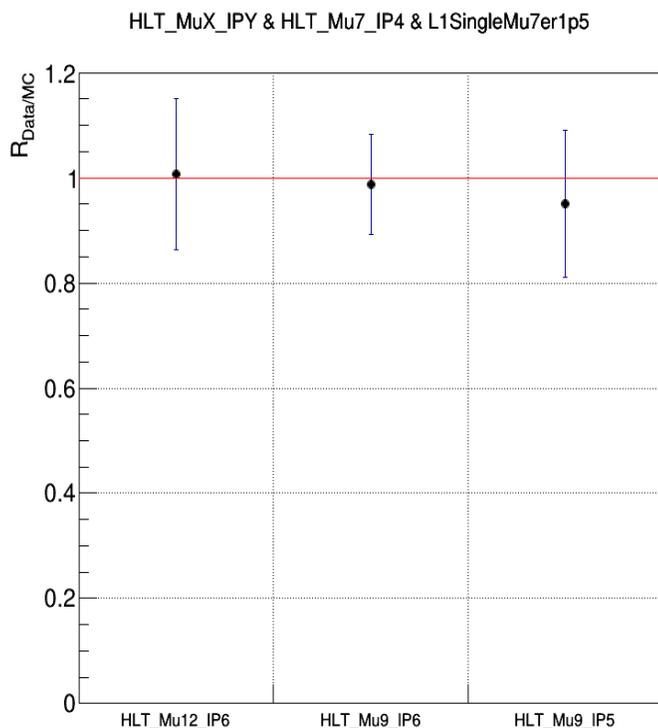| Lumi col. [E34]	Set0	Set1	Set2	Lumi col. [E34]	Set2 bis	Set3
1.6	-	-	HLT_Mu12_IP6	1.7	HLT_Mu12_IP6	HLT_Mu12_IP6
1.4	-	HLT_Mu9_IP6	HLT_Mu9_IP6	1.5	HLT_Mu9_IP6	HLT_Mu9_IP5
1.2	-	HLT_Mu9_IP6	HLT_Mu9_IP5	1.3	HLT_Mu9_IP5	HLT_Mu8_IP5
1	HLT_Mu9_IP6 HLT_Mu10p5_IP3p5 HLT_Mu8p5_IP3p5	HLT_Mu9_IP6	HLT_Mu9_IP5	1.1	HLT_Mu8_IP5	HLT_Mu7_IP4
0.8		HLT_Mu8_IP3	HLT_Mu7_IP4	0.9	HLT_Mu7_IP4	HLT_Mu7_IP4
First Fill	6659	6672	6762		7132	7271
Era	during 2018A	during 2018A	during 2018B		during 2018D	during 2018D
comments		6688 - 6690: incorrect prescales of L1 seeds	6762: incorrect prescales of L1 seeds			

$$R_{Data/_{MC}} = \frac{\epsilon_{Data}(HLT)}{\epsilon_{MC}(HLT)} = \frac{N_{B,Data}(HLT\_MuX\_IPY \& HLT\_Mu7\_IP4 \& L1T)/_{N_{B,Data}(HLT\_Mu7\_IP4 \& L1T)}}{N_{B,MC}(HLT\_MuX\_IPY \& HLT\_Mu7\_IP4 \& L1T)/_{N_{B,MC}(HLT\_Mu7\_IP4 \& L1T)}}$$

- $N_{B,Data}$ is obtained by taking yields from fits.
- To compare Data with MC, lumisections which all 4 HLT paths are turned-on is considered (Run2018D)

B+　　　　　　　　　　　　　　**Bs**　　　　　　　　　　　　　　**B0**

Source of Systematic Uncertainties

There are two categories of systematic uncertainties: correlated/uncorrelated bin-to-bin

1. **Source of uncertainties correlated bin-to-bin (global uncertainties):**
   - Uncertainty from **external inputs** (N_a, N_F, τ_{B^0}, $\tau_{B_s^0}$, and branching fractions)
   - Tracking efficiency:
     - **2.1% per track** estimated by tracking POG
     - Treated to be correlated bin-to-bin
   - BDT efficiency
     - Checked that it is independent of p_T or |y|
   - In B_s^0, uncertainty from Non-φ resonant background subtraction

2. **Source of uncertainties uncorrelated bin-to-bin:**
   - Statistical uncertainties of the Monte Carlo samples
   - Uncertainty from the **fit model shapes**
   - Uncertainty associated to **MC reweighting process**

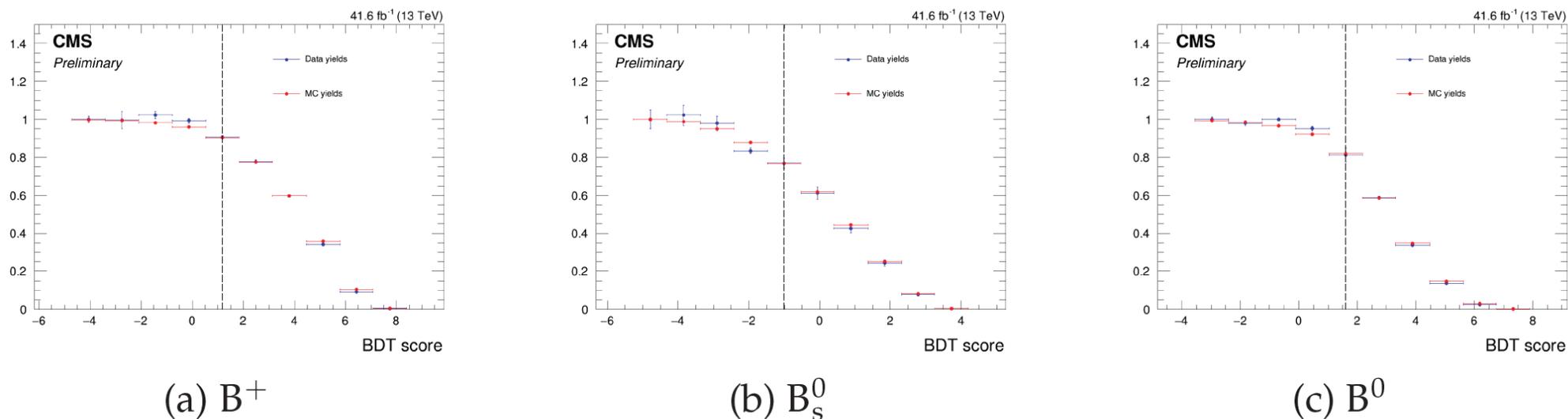| Source	f_s/f_u (%)	f_s/f_d (%)	f_d/f_u (%)
N_a, N_F	4.22	4.22	-
lifetime ratio	0.40	0.40	-
Branching fractions	5.36	4.03	5.46
Tracking efficiency	2.1	-	2.1
BDT performance	1.18	2.23	2.24
B_s^0 bkg subt.	0.9	0.9	-
Total global systematic uncertainty	7.4	6.3	6.3
Statistical uncertainty in simulation	1.7–3.1	2.2–3.7	2.1–3.6
Signal and Background shape	0.8–2.4	0.8–2.8	0.7–2.1
Reweighting in p_T and $|y|$	0.0–1.4	0.0–1.6	0.1–1.1
Total systematic uncertainty	< 8.7	< 7.8	< 7.8

Figure 19: BDT efficiencies in MC and data in all three channels. Yields are extracted from the fit in the invariant mass distribution with BDT scores above each bin centers.

As we have different BDTs for different channels, we cannot assume that the data/MC disagreement is canceled out in the final results.

- The difference of BDT efficiencies between data to MC is compared in all three channels.

The differences are considered as an uncertainty from each trained BDTs for the corresponding channel.

- The uncertainties which is not canceled in PFR is assigned as the systematic uncertainty associated with the BDT procedure.

The one of the goals of this analysis is to check pT dependence of PFRs

- Variables used for BDT training can be correlated with B meson's pT or |y|
- Then can bias a trend of PFR in pT or |y| after BDT threshold

BDT cut efficiency = N(BDT + pre-selection)/N(pre-selection)

➢ Different BDT cut efficiency bin-to-bin(combinatorial bkg more pronounced in low pT), but its impact on the efficiency ratio(or PFR) is constant

In B+ channel, we collect the opposite signs of π

- charged hadron tracks can be misidentified as muon pair from J/Psi

m($\pi^+\pi^-$) distribution with muon mass assigned to both tracks instead of pion mass is presented

- No J/Psi contribution seen ~ 3 GeV

check for J/Ψ peak in B$^+ \to$ Kππ decay channel

mass	
Entries	191815
Mean	3.037
Std Dev	0.286

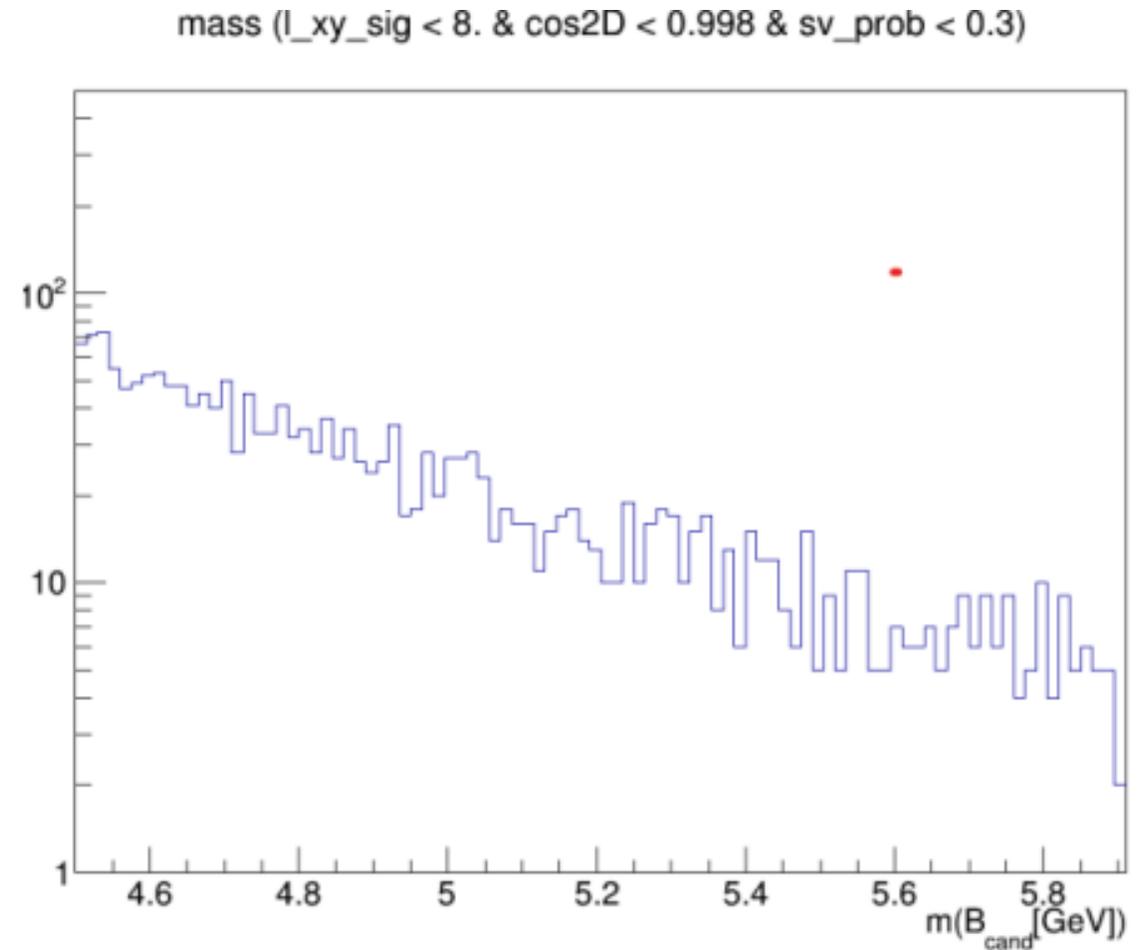m(ππ)[GeV] with μ mass assigned to both tracks

MC samples:
- Muon filter: requires 3 truth-level muon, at least one with $p_T > 5$ GeV
- Probe filter: requires the presence of a third "bachelor" muon not from J/Ψ. $p_T > 5$ GeV, $|\eta| < 2.5$
- 3 central MC samples per channel:
    1) Require B hadron decay according to the decay chain of interest
    2) Require B hadron decay wit the muon filter
    3) Require B hadron decay with the probe filter

Data set name	Events
/BdToKstarJpsi_ToKPiMuMu_probefilter_SoftQCDnonD_TuneCP5_13TeV-pythia8-evtgen/RunIIAutumn18MiniAOD-PUPoissonAve20_BParking_102X_upgrade2018_realistic_v15_ext1-v1/MINIAODSIM	5M
/BdToJpsiKstar_SoftQCDnonD_TuneCP5_13TeV-pythia8-evtgen/RunIIAutumn18MiniAOD-102X_upgrade2018_realistic_v15-v2/MINIAODSIM	500K
/BsToPhiJpsi_ToKKMuMu_probefilter_SoftQCDnonD_TuneCP5_13TeV-pythia8-evtgen/RunIIAutumn18MiniAOD-PUPoissonAve20_BParking_102X_upgrade2018_realistic_v15-v3/MINIAODSIM	340K
/BsToPhiJpsi_ToKKMuMu_probefilter_SoftQCDnonD_TuneCP5_13TeV-pythia8-evtgen/RunIIAutumn18MiniAOD-PUPoissonAve20_BParking_102X_upgrade2018_realistic_v15_ext1-v1/MINIAODSIM	2M
/BsToJpsiPhi_SoftQCDnonD_TuneCP5_13TeV-pythia8-evtgen/RunIIAutumn18MiniAOD-102X_upgrade2018_realistic_v15-v2/MINIAODSIM	500K
/BuToKJpsi_ToMuMu_probefilter_SoftQCDnonD_TuneCP5_13TeV-pythia8-evtgen/RunIIAutumn18MiniAOD-PUPoissonAve20_BParking_102X_upgrade2018_realistic_v15-v2/MINIAODSIM	2.2M
/BuToJpsiK_SoftQCDnonD_TuneCP5_13TeV-pythia8-evtgen/RunIIAutumn18MiniAOD-102X_upgrade2018_realistic_v15-v2/MINIAODSIM	500K
($B^{\pm} \to \pi^{\pm}J/\psi(1S)$ from private MC)	50K

Table 5: MC samples used in this analysis.

Charmonium: Validity of approach 'mass closest to K*'

- The invariant mass distribution of B0 is presented under conditions where signals are not expected to exist (purely combinatorial).
  - There is no artificially created peak in the distribution. Therefore, it appears that the approach of selecting the K* candidate "closest to the K* mass" is valid, with little risk of creating any artificial peaks around the signals.

mass (l_xy_sig < 8. & cos2D < 0.998 & sv_prob < 0.3)

Efficiency determination

The efficiencies for the three channels are determined

- **Tag**: μ filter requires **3 truth-level muon**, at least one with p_T > 5 GeV
- **Probe**: μ filter requires **the presence of a third "bachelor" muon not from J/Ψ**
  - p_T > 5 GeV, $|\eta|$ < 2.5
- **Filter efficiencies are not included in total efficiency**
  - These are canceled out in the PFR

MC samples are reweighted

- **Tag side**: **FONLL vs PYTHIA** comparison
- **Probe side**: **MC vs Data from hadronic open-charm**

Muon Trigger Scale factor is applied

- Only on tag-side events
  - Probe-side is minimally biased by triggers
- Computed on the unique set of triggers of this analysis
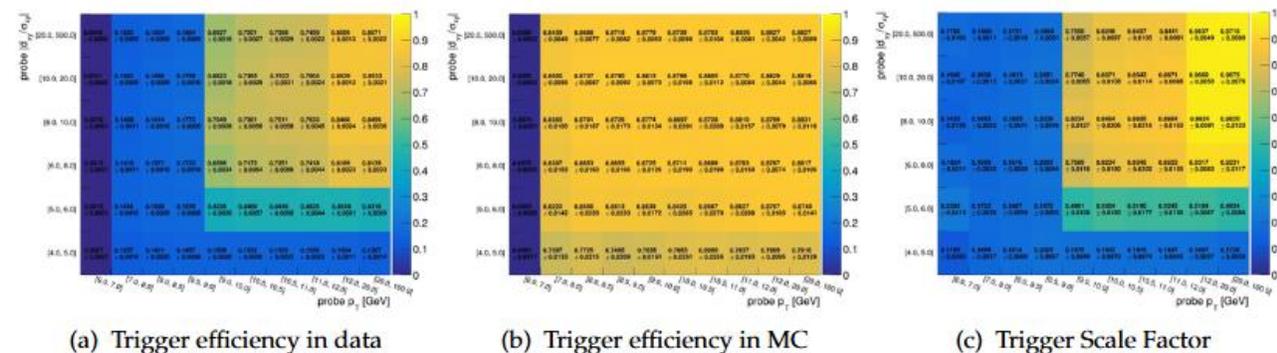
Comparison of PYTHIA versus FONLL in p_T, $|y|$

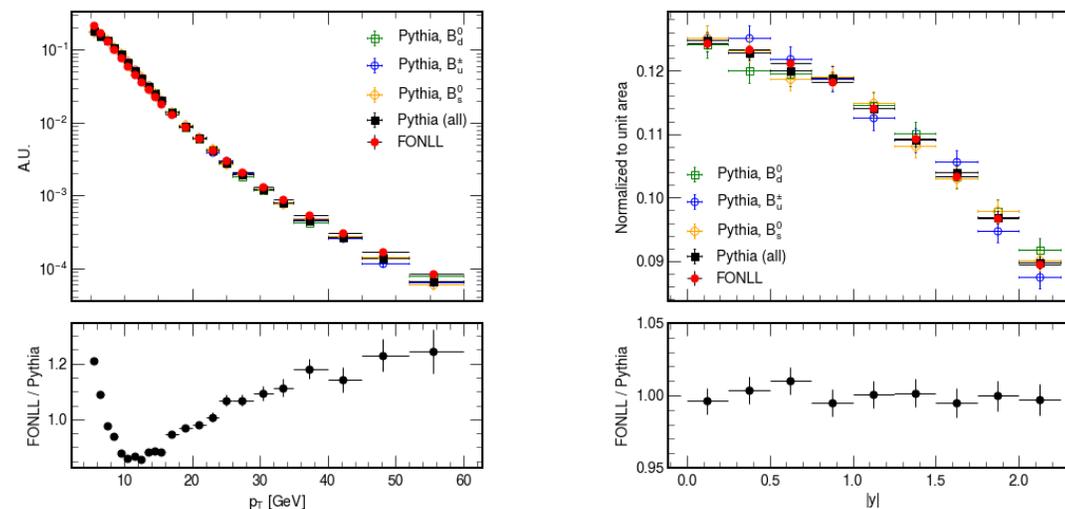

(a) Trigger efficiency in data (b) Trigger efficiency in MC (c) Trigger Scale Factor

Figure 7: Trigger efficiencies and scale factors in bins of the probe muon p_T and $|d_{xy}/\sigma_{xy}|$ for the full B-parking dataset.

(a) Efficiency vs. p_T

(b) Efficiency vs. $|y|$
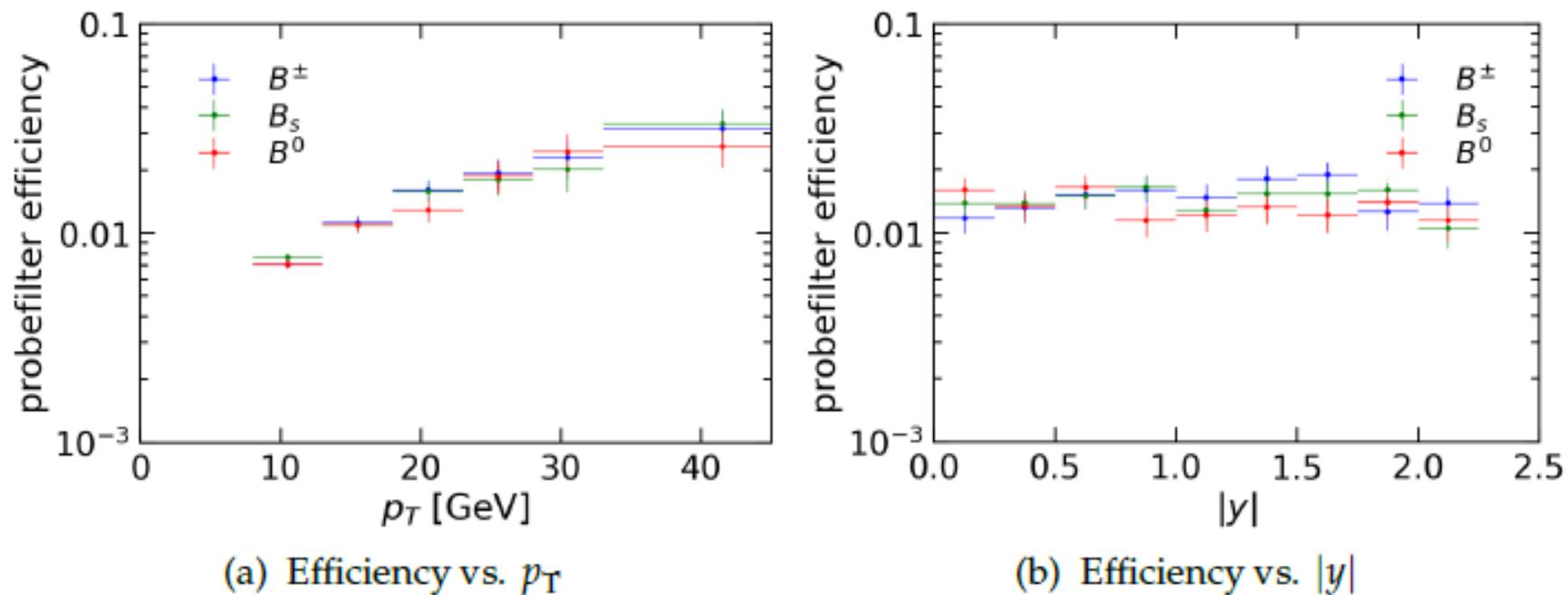
Figure 16: Probefilter efficiencies derived by emulating the probefilter on inclusive samples.
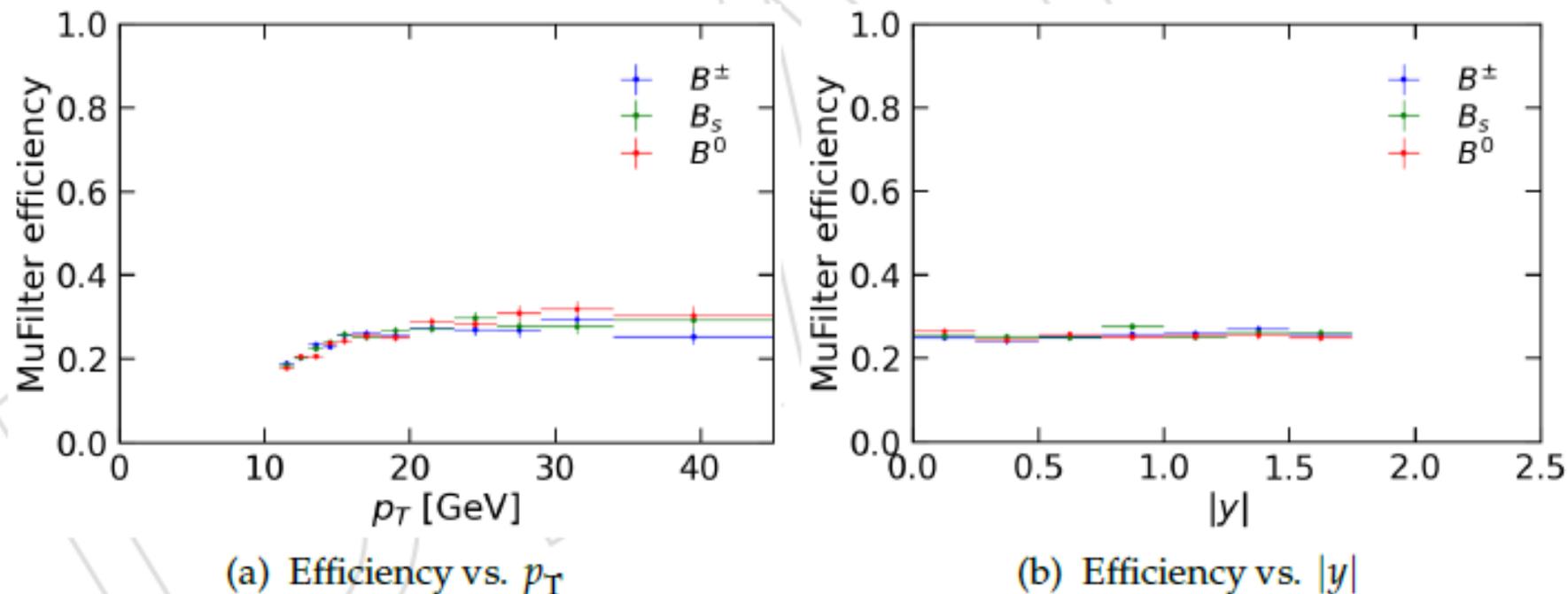
(a) Efficiency vs. p_T

(b) Efficiency vs. $|y|$

Figure 15: Mufilter efficiencies derived by emulating the Mufilter on inclusive samples.

Source of Systematic Uncertainties

1. **Source of uncertainties correlated bin-to-bin:**
   - Tracking efficiency
     - **2.1% per track** estimated by <u>tracking POG</u>
   - The uncertainty of branching fractions for f_d/f_u
     - **5.1%** for the branching fraction ratio

Source	Tag			Probe		
	$\mathcal{R}_s$ (%)	$\mathcal{R}_s^d$ (%)	f_d/f_u (%)	$\mathcal{R}_s$ (%)	$\mathcal{R}_s^d$ (%)	f_d/f_u (%)
Statistical uncertainty in simulation	0.7–6.7	0.8–9.3	0.7–7.2	1.9–4.9	1.7–4.8	1.6–4.2
Signal and Background shape	0.8–4.7	0.6–5.2	0.5–4.2	1.3–7.9	1.1–6.4	0.9–6.4
Trigger SF	1.9–2.6	1.9–2.7	1.9–2.7	-	-	-
Reweighting in p_T and $|y|$	0.0–5.3	0.0–4.3	0.0–6.5	0.0–3.7	0.0–3.8	0.0–4.9
Total systematic uncertainty	<8.5	<9.8	< 8.8	<10.0	<8.1	<7.7

2. **Source of uncertainties uncorrelated bin-to-bin:**
   - Statistical uncertainties of MC samples
   - Uncertainty from the **fit model**
     - Estimated by changing shapes of fit models to alternative shapes
   - Uncertainty associated to **MC reweighting process**
     - **Tag**: FONLL vs PYTHIA
     - **Probe**: MC vs Data
   - Uncertainty associated to **Trigger SF**
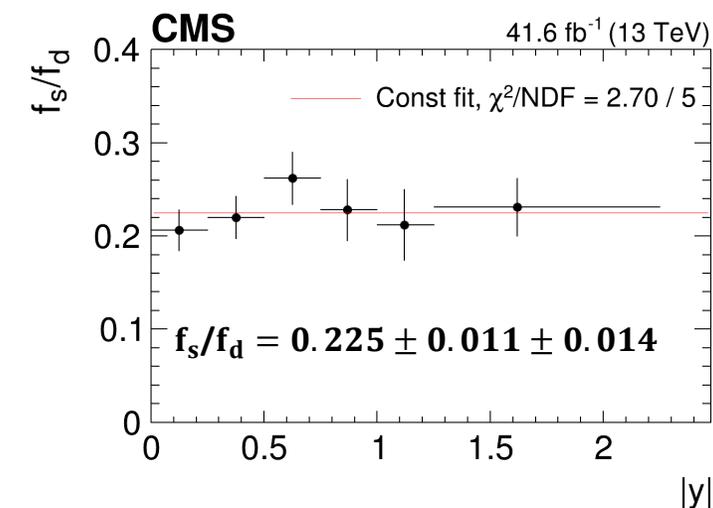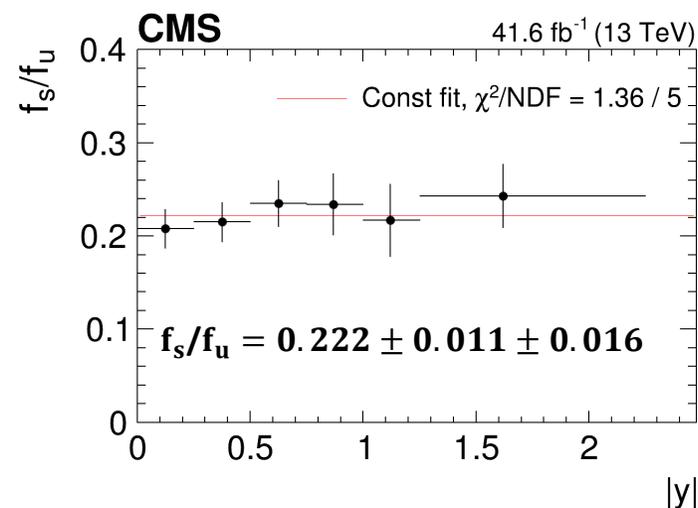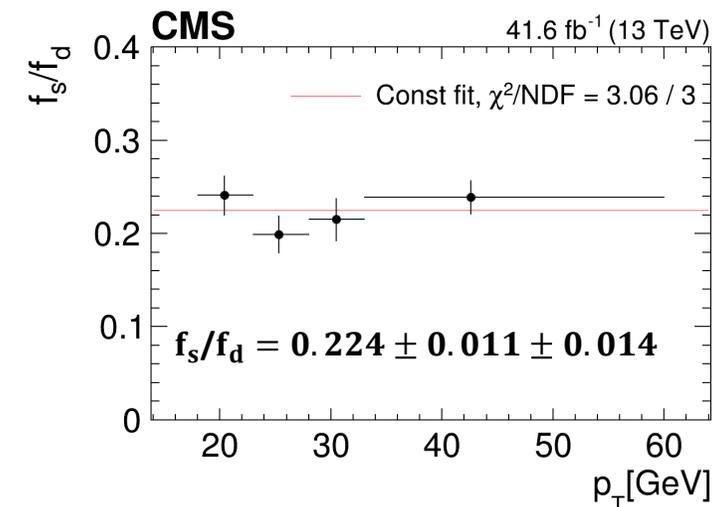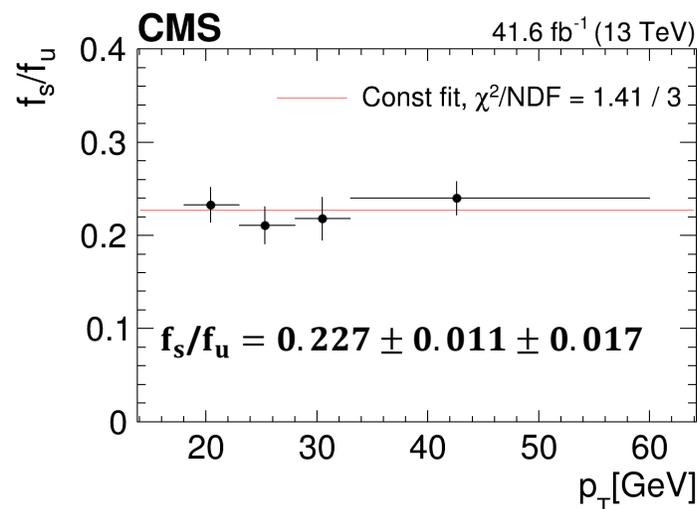   - varying SF up and down by its uncertainty

Previous CMS study showed that PFRs are asymptotically flat at high p_T

- $p_T > 18$ GeV
- PRL 131 (2023) 121901

The absolute normalization of PFRs

- f_s/f_d at LEP : 0.249 ± 0.023
  - HFLAV: EPJC 81 (2021) 226
  - approximate p_T of 40 GeV in Z decays

- f_s/f_d at LHCb : 0.2539 ± 0.0079 (13 TeV)
  - LHCb: PRD 104 (2021) 032005
  - $p_T \in [1.5, 40]$ GeV

- The recent BMM measurement in CMS
  - PLB 842 (2023) 137955
  - $f_s/f_u^{eff} = 0.231 \pm 0.008$
  - p_T weighted average of LHCb measurement in their phase space

CMS   41.6 fb⁻¹ (13 TeV)
Const fit, χ^2/NDF = 1.41 / 3
$f_s/f_u = 0.227 \pm 0.011 \pm 0.017$

CMS   41.6 fb⁻¹ (13 TeV)
Const fit, χ^2/NDF = 3.06 / 3
$f_s/f_d = 0.224 \pm 0.011 \pm 0.014$

CMS   41.6 fb⁻¹ (13 TeV)
Const fit, χ^2/NDF = 1.36 / 5
$f_s/f_u = 0.222 \pm 0.011 \pm 0.016$

CMS   41.6 fb⁻¹ (13 TeV)
Const fit, χ^2/NDF = 2.70 / 5
$f_s/f_d = 0.225 \pm 0.011 \pm 0.014$

f_{B^0}/f_{B^+} vs $f_{\overline{B}^0}/f_{B^-}$

- **Combined** f_{B^0}/f_{B^+} **= 0.97 ± 0.05**
- **Combined** $f_{\overline{B}^0}/f_{B^-}$ **= 0.98 ± 0.05**
- f_{B^0}/f_{B^+} and $f_{\overline{B}^0}/f_{B^-}$ are consistent with **each other within a 3% precision**
    - Considering correlated systematic uncertainty
    - Supporting **CP symmetry in B^+ and B^0 production**

Conversion of $\mathcal{R}$ to PFR

Combined results of charmonium and hadronic open-charm analysis on probe-side

- pT $\in$ [8.0, 50.0) GeV and |y| $\in$ [0, 2.25)

$$\frac{\mathcal{B}(B^{\pm}\to J/\psi(1S)K^{\pm})}{\mathcal{B}(B^{\pm}\to\pi^{\pm}\overline{D}^0)} = \frac{N_{corr}(B^{\pm}\to J/\psi(1S)K^{\pm})}{N_{corr}(B^{\pm}\to\pi^{\pm}\overline{D}^0)}\frac{\mathcal{B}(\overline{D}^0\to K^+\pi^-)}{\mathcal{B}(J/\psi(1S)\to\mu\mu)} = 0.210 \pm 0.008$$

(PDG: 0.218 $\pm$ 0.008)

$$\frac{\mathcal{B}(B_s^0\to J/\psi(1S)\phi)}{\mathcal{B}(B_s^0\to\pi^+ D_s^-)} = \frac{N_{corr}(B_s^0\to J/\psi(1S)\phi)}{N_{corr}(B_s^0\to\pi^+ D_s^-)}\frac{\mathcal{B}(D_s^-\to\phi\pi^-)}{\mathcal{B}(J/\psi(1S)\to\mu\mu)} = 0.357 \pm 0.024$$

(PDG: 0.362 $\pm$ 0.032)

$$\frac{\mathcal{B}(B^0\to J/\psi(1S)K^*(892))}{\mathcal{B}(B^0\to\pi^+ D^-)} = \frac{N_{corr}(B^0\to J/\psi(1S)K^*(892))}{N_{corr}(B^0\to\pi^+ D^-)}\frac{\mathcal{B}(D^-\to K^+\pi^-\pi^-)}{\mathcal{B}(K^*\to K\pi)\mathcal{B}(J/\psi(1S)\to\mu\mu)} = 0.478 \pm 0.018$$

(PDG: 0.506 $\pm$ 0.026)

The measured B_s and B^0 branching fraction ratios improve on the PDG precision

$B^{\pm}$ ratio is as good as the world average